iScience

CellPress
OPEN ACCESS

Article

A Neuroligin-1 mutation associated with Alzheimer's disease produces memory and age-dependent impairments in hippocampal plasticity

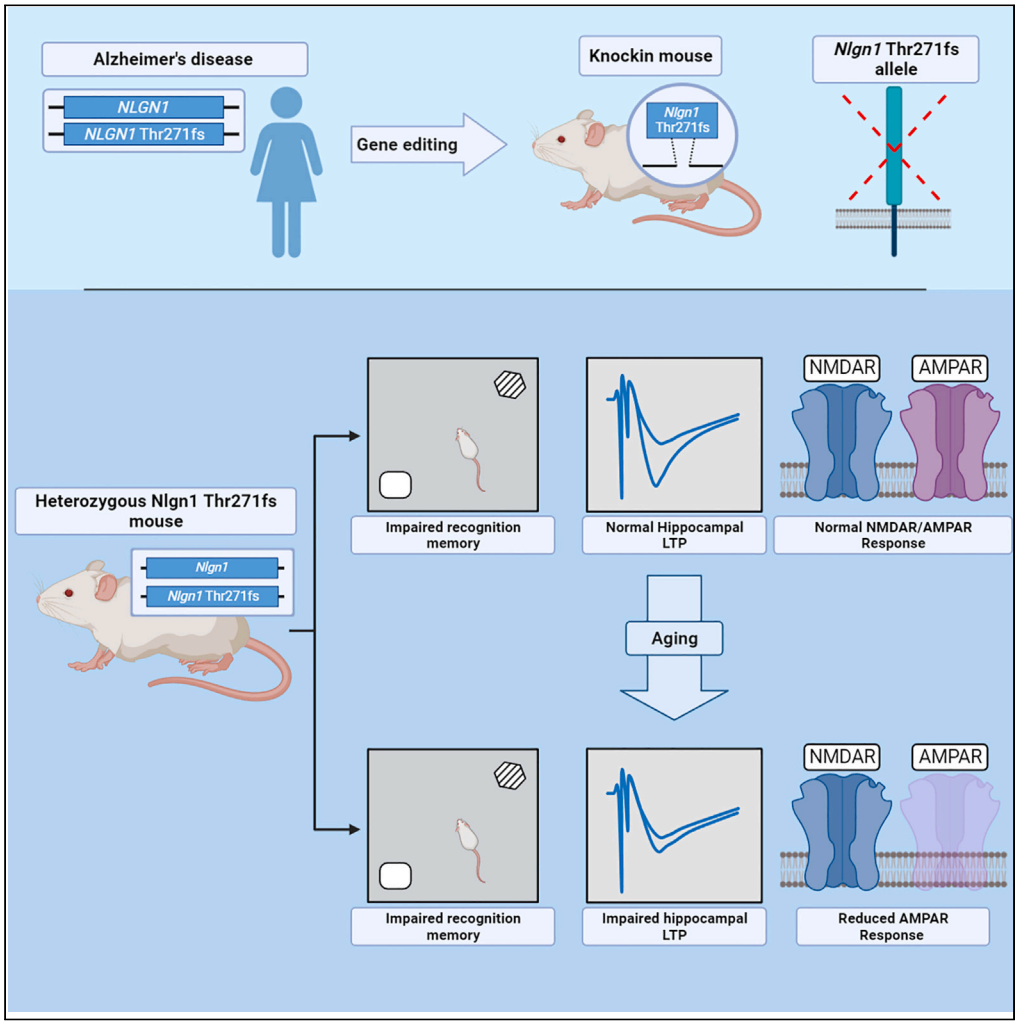

Francisco Arias-Aragón, Enriqueta Tristán-Clavijo, Irene Martínez-Gallego, ..., Antonio Rodríguez-Moreno, Amalia Martinez-Mir, Francisco G. Scholl

fgs@us.es

Highlights

Sustained Nlgn1 decrease in the AD-associated Nlgn1 Thr271fs heterozygous (HTZ) mouse

Short-lived recognition memory in HTZ Nlgn1 Thr271fs mouse

Age-dependent decrease in hippocampal LTP in HTZ Nlgn1 Thr271fs mouse

Age-dependent loss of AMPAR-mediated synaptic responses in HTZ Nlgn1 Thr271fs mouse

Arias-Aragón et al., iScience 26, 106868
June 16, 2023
https://doi.org/10.1016/j.isci.2023.106868

iScience

CellPress
OPEN ACCESS

Article

A Neuroligin-1 mutation associated with Alzheimer's disease produces memory and age-dependent impairments in hippocampal plasticity

Francisco Arias-Aragón,[1,2] Enriqueta Tristán-Clavijo,[1,4,5,7] Irene Martínez-Gallego,[3,7] Estefanía Robles-Lanuza,[1,2,7] Heriberto Coatl-Cuaya,[3] Celia Martín-Cuevas,[1,2,6] Ana C. Sánchez-Hidalgo,[1,2,6] Antonio Rodríguez-Moreno,[3] Amalia Martinez-Mir,[1] and Francisco G. Scholl[1,2,8,*]

SUMMARY

Alzheimer's disease (AD) is characterized by memory impairments and age-dependent synapse loss. Experimental and clinical studies have shown decreased expression of the glutamatergic protein Neuroligin-1 (Nlgn1) in AD. However, the consequences of a sustained reduction of Nlgn1 are unknown. Here, we generated a knockin mouse that reproduces the *NLGN1* Thr271fs mutation, identified in heterozygosis in a familial case of AD. We found that *Nlgn1* Thr271fs mutation abolishes Nlgn1 expression in mouse brain. Importantly, heterozygous Nlgn1 Thr271fs mice showed delay-dependent amnesia for recognition memory. Electrophysiological recordings uncovered age-dependent impairments in basal synaptic transmission and long-term potentiation (LTP) in CA1 hippocampal neurons of heterozygous Nlgn1 Thr271fs mice. In contrast, homozygous Nlgn1 Thr271fs mice showed impaired fear-conditioning memory and normal basal synaptic transmission, suggesting unshared mechanisms for a partial or total loss of Nlgn1. These data suggest that decreased Nlgn1 may contribute to the synaptic and memory deficits in AD.

INTRODUCTION

Cognitive function relies on the correct transfer of information between neurons through an intricate network of synaptic connections. Extensive work on the Alzheimer's disease (AD) field supports the hypothesis that the memory deficits exhibited by AD patients stem from synaptic failure, which may be caused by the early loss of synaptic components.[1–3] The relatively large time period preceding the full expression of AD symptoms may reflect the temporal progression of the underlying pathological mechanisms. This time period is particularly evident in cases of familial AD (FAD), where carriers of fully penetrant heterozygous mutations in FAD-linked genes develop AD after decades of life.[4] Although the age-dependence for the expression of full symptoms poses experimental challenges when searching for pathogenic mechanisms in AD, the functional validation of candidates for synaptic and memory impairments may widen the clinical opportunities at earlier phases of AD.

Neuroligins (NLGN1, NLGN2, NLGN3, NLGN4X, and NLGN4Y) form a family of postsynaptic cell-adhesion proteins associated with brain diseases.[5] The initial identification of point and frameshift mutations in *NLGN3* and *NLGN4X* genes in autism supported a role for a neuroligins (Nlgns) dysfunction in neurodevelopmental disorders.[6,7] However, the role of *NLGN1* in disease has been scarce; despite Nlgn1 being a main component of glutamatergic terminals expressed at relatively high levels than other Nlgn family members.[8–10] At glutamatergic synapses, Nlgn1 can recruit alpha-amino-3-hydroxy-5-methyl-4-isoxazolepropionic acid (AMPA) (AMPARs) and N-methyl-D-aspartate (NMDA) receptors (NMDARs) through interactions mediated by the intracellular and extracellular domains, respectively.[11–15] Moreover, it has been recurrently reported that the loss of Nlgn1 by knockout or knockdown approaches produces a reduction in long-term potentiation (LTP) accompanied by a major decrease in NMDAR-mediated synaptic currents.[11,16–20] Since LTP is thought to underlie the physiological processes associated with learning and memory,[21,22] loss of Nlgn1 might mediate synaptic dysfunction and cognitive decline in brain diseases.

Recent data support a role for reduced Nlgn1 function in AD. Studies in human samples have found decreased levels of Nlgn1 in the brain of AD patients.[23,24] In one study, Goetzl et al. found Nlgn1 reduction in plasma

[1]Instituto de Biomedicina de Sevilla (IBiS), Hospital Universitario Virgen del Rocío/CSIC/Universidad de Sevilla, 41013 Seville, Spain

[2]Departamento de Fisiología Médica y Biofísica, Universidad de Sevilla, 41009 Seville, Spain

[3]Laboratory of Cellular Neuroscience and Plasticity, Department of Physiology, Anatomy and Cell Biology, University Pablo de Olavide, 41013 Seville, Spain

[4]Present address: Departamento de Medicina, Universidad de Sevilla/CSIC, 41009 Seville, Spain

[5]Present address: CIBERINFEC, ISCII

[6]Present address: CIBERSAM, ISCIII (Spanish Network for Research in Mental Health)

[7]These authors contributed equally

[8]Lead contact

*Correspondence: fgs@us.es

https://doi.org/10.1016/j.isci.2023.106868

neuron-derived exosomes of pre-symptomatic patients years before the diagnosis of dementia.[25] The reduction of Nlgn1 function in AD might originate from genetic and non-genetic mechanisms. Thus, it has been shown that Nlgn1 is a target for amyloid beta (Abeta) peptides, the main component of plaques associated with AD, and hindering the Nlgn1-Abeta interaction prevents from the synaptotoxic effects caused by Abeta in mouse brain.[26,27] In addition to these post-transcriptional mechanisms, Nlgn1 levels could decrease in AD by an epigenetic mechanism, as it was shown in rat brain upon acute injection of Abeta.[28] However, it is currently not known whether the decrease in Nlgn1 plays a direct pathological role in the synaptic and memory deficits associated with AD or, rather, its reduction reflects the broader loss of synapses occurring in the disease. The consequences of a specific loss of Nlgn1 in memory function have been studied in juvenile and young adult rodents by knockout and knockdown approaches. Thus, it has been reported that Nlgn1 knockout (KO) mice showed early deficits in hippocampal LTP and spatial memory, whereas fear-conditioning memory was not affected.[16] By contrast, in another study fear-conditioning memory was reduced in rats upon acute downregulation of Nlgn1 in the amygdala by shRNA injection.[19] These findings suggest not only that a specific loss of Nlgn1 can indeed affect memory function but also denote that differences in the experimental approaches affecting the extent, duration or levels leading to the Nlgn1 reduction likely alter the functional outcome. It is important to stress that work in mouse models and AD patients have identified a partial reduction of Nlgn1, the consequences of which may differ from the total or near-total inhibition of expression produced by knockout and knockdown methodologies. However, the prolonged effect of a partial reduction of Nlgn1, as it would occur in heterozygous Nlgn1 KO mice, has not been reported. Importantly, knockout approaches are often prone to compensatory mechanisms during development that can modify the phenotype in the adulthood.[29] Therefore, it is not known if an AD-associated reduction of Nlgn1 produces impairments in memory and synaptic function. Answering these questions requires the lifelong characterization of a sustained Nlgn1 reduction in animal models with construct validity.

In this study, we have generated a knockin mouse that reproduces a frameshift mutation in the *NLGN1* gene previously identified in heterozygosis in AD.[30] We found that the Thr271fs mutation generates a null *Nlgn1* allele, which produces a partial (50%) expression of Nlgn1 protein in the heterozygous (HTZ) mutant mice. Importantly, HTZ Nlgn1 Thr271fs mice exhibit persistent delay-dependent amnesia for recognition memory, failing to recognize new objects presented after a long delay, but not at short delays. Electrophysiological recordings in CA1 hippocampal neurons of HTZ Nlgn1 Thr271fs mice uncovered age-dependent deficits in basal synaptic transmission and synaptic plasticity such as LTP, which are detected in middle-aged and old individuals, but are absent in young adult mice. Moreover, AMPAR-currents are specifically decreased in old but not young CA1 neurons of HTZ Nlgn1 Thr271fs mice, whereas NMDAR-currents are not affected. Strikingly, homozygous (HMZ) Nlgn1 Thr271fs mice present distinct memory and behavioral deficits and decreased hippocampal LTP at a young adult age, but normal synaptic strength through life. Our data indicate that a chronic and partial loss of Nlgn1 produces specific memory deficits and age-dependent loss of synaptic transmission and plasticity and that Nlgn1 Thr271fs mouse may be a useful patient-based model for studying AD.

RESULTS

Generation of Nlgn1 Thr271fs knockin mice

Previously, we had identified a heterozygous TT insertion in the *NLGN1* gene in a familial case of AD.[30] The sequence of the affected region is conserved in human and mouse genomes (Figure 1A). In order to understand the consequences of the AD-associated *NLGN1* Thr271fs mutation, we used the TALENS system to introduce the Thr271fs mutation into the mouse *Nlgn1* gene. The donor DNA contains the two inserted TT nucleotides along with a silent mutation to create an *Hpa*I restriction site as to facilitate detection of the mutant allele (Figure 1B). Genomic PCR with *Nlgn1* primers followed by *Hpa*I restriction identified three potential founder mice out of 20 newborn mice. Sanger sequencing confirmed heterozygosis of the mutant *Nlgn1* Thr271fs allele in two founder mice (Figure 1C), whereas the third founder contained an additional downstream deletion in the second *Nlgn1* allele, and it was thus discarded. Breeding of the two founder lines with C57BL/6J mice showed propagation of the edited *Nlgn1* Thr271fs allele to the progeny with the expected 50% frequency. Genomic qPCR in the progeny of the two Nlgn1 Thr271fs mouse lines discarded off-target insertion of the donor DNA. Therefore, we selected one of the two identical-edited Nlgn1 Thr271fs mouse lines for further research.

The AD-associated *Nlgn1* Thr271fs mutation produces a null *Nlgn1* allele

The *Nlgn1* Thr271fs mutation is expected to translate into a C-terminally truncated Nlgn1 fragment of 27 kDa.[30] However, frameshift mutations are often prone to post-transcriptional silencing by a

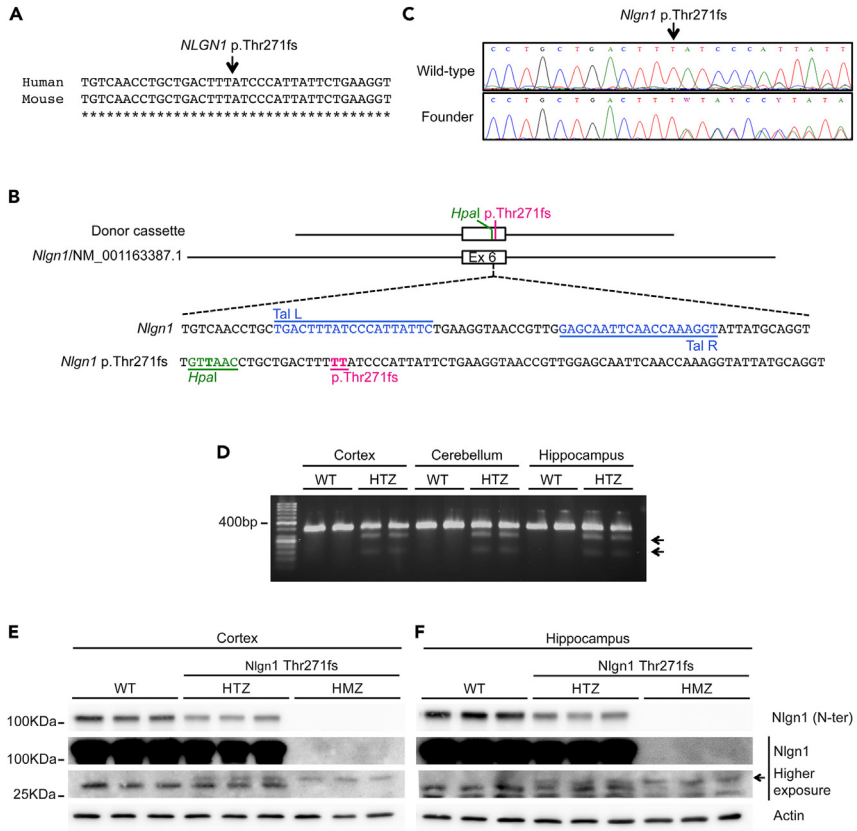

Figure 1. Generation of the Nlgn1 Thr271fs mouse and expression of the mutant *Nlgn1* Thr271fs allele in brain

(A) Sequence conservation of human *NLGN1* and mouse *Nlgn1* genes. The Thr271 residue is indicated.

(B) Schematic drawing showing the knockin strategy. The inserted TT and the *HpaI* site are indicated in the donor DNA.

(C) Nucleotide sequence of the edited Nlgn1 Thr271fs mutation is shown in comparison with the wild-type allele.

(D) RT-PCR experiments from brain tissues of wild-type and HTZ Nlgn1 Thr271fs mice. Incubation with *HpaI* produced a digestion-resistant band expressed from the wild-type *Nlgn1* allele and two digested bands from the edited *Nlgn1* Thr271fs allele, indicated with arrows. Note the low intensity of the bands produced by the *Nlgn1* Thr271fs allele.

(E and F) Western-blot experiments from cortical (E) and hippocampal (F) lysates of wild-type and Nlgn1 Thr271fs mice. The Nlgn1 antibody recognizes an N-terminal epitope located 5′ upstream of the TT insertion site in the mutant *Nlgn1* allele. Nlgn1 protein is not produced by the *Nlgn1* Thr271fs allele. ((E) One-way ANOVA with Holm-Sidak's post-hoc analysis. $F_{(2,6)} = 287.2$, $p < 0.0001$, wild-type vs. HTZ $p < 0.0001$, wild-type vs. HMZ $p < 0.0001$, HTZ vs. HMZ $p < 0.0001$. Wild-type 1 $\pm$ 0.04; HTZ 0.516 $\pm$ 0.02; HMZ 0.001 $\pm$ 0.0004. (F) One-way ANOVA with Holm-Sidak's post-hoc analysis. $F_{(2,6)} = 129.6$, $p < 0.0001$, wild-type vs. HTZ $p = 0.0003$, wild-type vs. HMZ $p < 0.0001$, HTZ vs. HMZ $p = 0.0003$. Wild-type 1 $\pm$ 0.05; HTZ 0.541 $\pm$ 0.053; HMZ 0.001 $\pm$ 0.0003). Fractional amounts of an N-terminal Nlgn1 fragment is detected in lysates of Nlgn1 Thr271fs mice in cases of overexposed blots, indicated with arrows. See also Figure S1. Data are represented as mean $\pm$ SEM.

nonsense-mediated mRNA decay mechanism. To analyze the expression of the *Nlgn1* Thr271fs allele we first performed RT-PCR experiments in brain tissues followed by *Hpa*I digestion. In wild-type mice, *Hpa*I did not cut the amplified Nlgn1 PCR fragment, as expected for the unedited *Nlgn1* allele (Figure 1D). In HTZ Nlgn1 Thr271fs mice digestion with *Hpa*I resulted in two bands of the expected size for the edited allele, along with a wild-type *Nlgn1* band resistant to *Hpa*I restriction (Figure 1D). Notably, the bands corresponding to the *Nlgn1* Thr271fs allele were of much lower intensity than the band obtained from the wild-type *Nlgn1* allele in the different brain regions analyzed. These data suggest that the mRNA transcribed from the *Nlgn1* Thr271fs allele is unstable and mostly degraded. To further confirm that the *Nlgn1* Thr271fs mutation generates a null allele, we performed Western-blot experiments using an antibody against the N-terminal domain of Nlgn1 (Figures 1E and 1F). The expression of Nlgn1 protein decreased by half in HTZ Nlgn1 Thr271fs mice, while it was absent in HMZ Nlgn1 Thr271fs mice, confirming the specificity of the Nlgn1 antibody. Nlgn1 protein levels in wild-type mice and the decrease in HTZ Nlgn1 Thr271fs

mice were similar in male and female individuals (Figure S1). These results are consistent with a lack of expression of Nlgn1 protein from the AD-associated mutation. Moreover, the truncated N-terminal Nlgn1 fragment was only marginally detected in overexposed blots of Nlgn1 Thr271fs mice (Figures 1E and 1F). The estimated level of the truncated Nlgn1 fragment was less than 1% of the mature Nlgn1 protein encoded by the wild-type allele in HTZ Nlgn1 Thr271fs mice, although this value is most likely an over-estimation due to the high exposure of the blots. These data indicate that AD-associated *Nlgn1* Thr271fs mutation generates a null *Nlgn1* allele, along with a fractional amount of a truncated Nlgn1 fragment.

Behavioral characterization of Nlgn1 Thr271fs mice in neurodevelopmental-associated tests

The diagnosis of cognitive deficits in brain diseases relies mainly on clinical evaluation. Trying to uncover relevant behavioral phenotypes in the Nlgn1 Thr271fs mouse, we performed a battery of behavioral tests. For each test, we analyzed HTZ and HMZ Nlgn1 Thr271fs mice in parallel as to detect specific alterations caused by a protein-dosage effect. Because inherited frameshift and inactivating mutations in X-linked *NLGN3* and *NLGN4X* genes have been identified in male patients with autism and other neurodevelopmental disorders,[6,7] we first evaluated if a partial or total loss of Nlgn1 affects behavioral traits commonly related to neurodevelopmental disorders, such as locomotion, anxiety, repetitive behavior, and social interaction (Figure S2).

In the open field test, HTZ Nlgn1 Thr271fs mice traveled the same total distance and performed similar entries to the center area as wild-type mice (Figure S2A). However, HMZ Nlgn1 Thr271fs mice showed a slight increase in the traveled distance and in the number of entries to the center area, which reaches statistical significance when compared with HTZ Nlgn1 Thr271fs mice (Figure S2A). The self-grooming assay evaluates the time a mouse spends performing a stereotyped behavior, and it is often increased in mouse models of autism.[31,32] HMZ Nlgn1 Thr271fs mice almost doubled the self-grooming time compared with wild-type mice (Figure S2B). However, HTZ Nlgn1 Thr271fs mice showed similar self-grooming time than wild-type mice, although a trend to an increased time was detected (Figure S2B). Social interaction was evaluated in the three-chamber test, an arena that gives the tested mouse the chance to interact with an age- and sex-matched mouse or with an inanimate object.[33] Wild-type, HTZ, and HMZ Nlgn1 Thr271fs mice interact preferentially with the caged mouse rather than with the object, although HMZ Nlgn1 Thr271fs mice showed a slight reduction in the average time interacting with the mouse (Figure S2C). This non-significant slight decrease in social interaction of HMZ Nlgn1 Thr271fs mice was also detected using the social index, which computes the percentage of time that each individual mouse differentially interacts with the social stimulus (Figure S2C). The increase in self-grooming time and the subtle differences in social interaction of HMZ Nlgn1 Thr271fs mice resemble the previously reported deficits in Nlgn1 KO mice.[16] These experiments indicate the absence of neurodevelopmental-associated deficits in young adult mice upon a partial loss of Nlgn1, whereas the inhibition of Nlgn1 expression produces some degree of hyperactivity, an increase in stereotyped behavior and subtle deficits in social interaction.

Decreased fear-conditioning memory in homozygous, but not heterozygous, Nlgn1 Thr271fs mice

Memory loss is a hallmark of cognitive decline in AD. Therefore, we studied the outcome of the Nlgn1 Thr271fs mouse in different memory paradigms. Fear conditioning is a type of associative memory that is formed during the co-presentation of a neutral stimulus (a tone as the conditioned stimulus) with an aversive stimulus (a mild electric shock as the non-conditioned). A later exposure to the conditioned stimulus retrieves the expression of fear memory in the conditioned mouse in the form of a freezing response indicated by the absence of movements. During conditioning, HTZ and HMZ Nlgn1 Thr271fs mice showed similar freezing time than wild-type mice to the three tones presentation, indicating normal fear learning (Figure 2A). Exposure to the tone one day later produced a freezing response in HTZ Nlgn1 Thr271fs mice of similar duration than wild-type mice, indicating that a partial loss of Nlgn1 does not affect fear memory. By contrast, HMZ Nlgn1 Thr271fs mice showed a decreased freezing time to the tone (Figure 2A). HTZ and HMZ Nlgn1 Thr271fs mice showed similar reaction time in the hot plate, which was faster than wild-types (one-way ANOVA with Tukey's post-hoc analysis. $F_{(2,27)} = 5.477$, $p = 0.010$, wild-type vs. HTZ $p = 0.027$, wild-type vs. HMZ $p = 0.016$, HTZ vs. HMZ $p = 0.933$. Wild-type: 7.56 $\pm$ 0.30; HTZ Nlgn1 Thr271fs: 6.17 $\pm$ 0.37; HMZ Nlgn1 Thr271fs: 5.99 $\pm$ 0.40. Time in s. Wild-type, n = 10; HTZ Nlgn1 Thr271fs, n = 11; HMZ Nlgn1 Thr271fs, n = 9), suggesting that differences in sensory processing do not underlie the distinct response in fear memory of Nlgn1 Thr271fs mice. These data indicated that the null expression of Nlgn1 produces a decrease in associative fear memory in adult mice, which is preserved by a partial loss of Nlgn1.

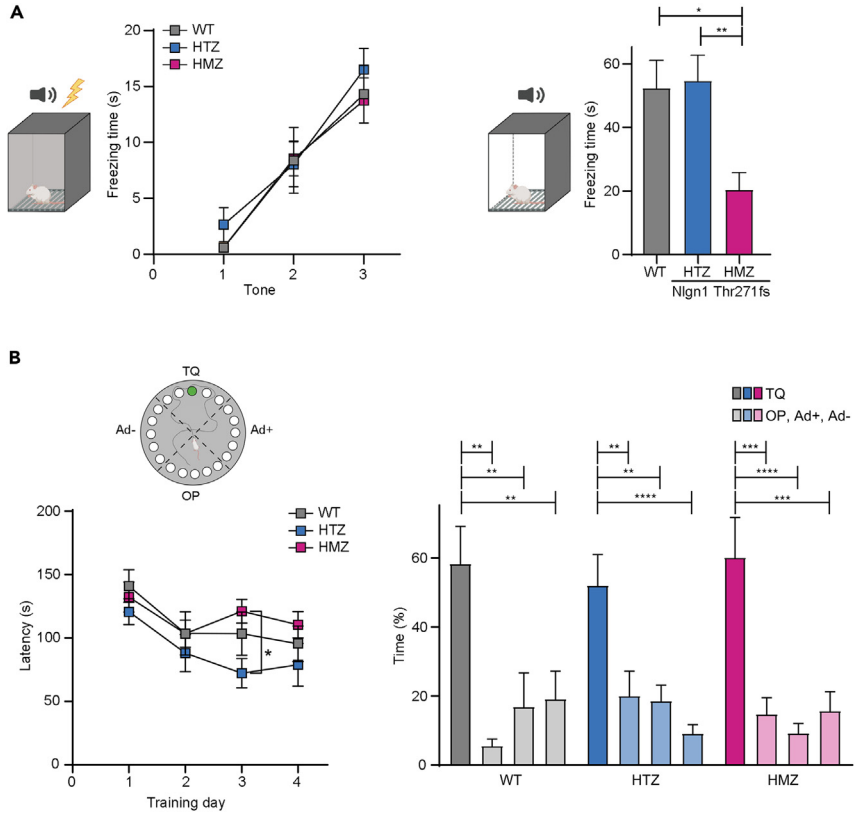

Figure 2. Decreased fear memory in HMZ Nlgn1 Thr271fs mice

(A) Fear conditioning. Freezing time during the conditioning session (left) (two-way repeated measures ANOVA with Tukey's post-hoc analysis on genotype. Interaction x genotype $F_{(4.50)} = 0.364$ p = 0.833; genotype $F_{(2.25)} = 0.341$ p = 0.714). Decreased freezing response (in s) during tone presentation in HMZ Nlgn1 Thr271fs (right) (one-way ANOVA with Tukey's post-hoc analysis. $F_{(2.25)} = 6.24$, p = 0.0063, wild-type vs. HTZ p = 0.974, wild-type vs. HMZ p = 0.0195, HTZ vs. HMZ p = 0.0099. Wild-type 52.32 ± 8.75; HTZ 54.61 ± 8.07; HMZ 20.40 ± 5.39). Wild-type, n = 9; HTZ, n = 10; HMZ, n = 9.

(B) Spatial memory in the Barnes Maze. Time (s) latency to find the escape hole during the four training sessions (left) (two-way repeated measures ANOVA with Tukey's post-hoc analysis on genotype. Interaction x genotype $F_{(6.108)} = 0.4359$ p = 0.853; genotype $F_{(2.108)} = 4.43$ p = 0.014. P-value< 0.05: HTZ vs. HMZ on training day 3 p = 0.034. Wild-type 140.85 ± 12.97, 103.50 ± 17.02, 103.35 ± 17.05, 95.46 ± 14.09; HTZ 120.68 ± 10.29, 88.00 ± 14.75, 72.25 ± 11.47, 78.84 ± 16.89; HMZ 132.30 ± 11.91, 103.44 ± 10.65, 121.11 ± 9.33, 110.44 ± 10.41). Percentage of time spent in quadrants (Ad-, TQ, Ad+, OP) one day after training (right). Differences compared with time spent in TQ within genotype (one-way ANOVA with Dunnett's multiple comparisons test analysis. WT: $F_{(3.36)} = 7.509$, p = 0.0005, TQ vs. OP p = 0.002, TQ vs. Ad+ p = 0.0036, TQ vs. Ad-p = 0.0061. HTZ: $F_{(3.40)} = 8.93$, p = 0.0001, TQ vs. OP p = 0.0024, TQ vs. Ad+ p = 0.0015, TQ vs. Ad-p < 0.0001. HMZ: $F_{(3.32)} = 11.53$, p < 0.0001, TQ vs. OP p = 0.0002, TQ vs. Ad+ p < 0.0001, TQ vs. Ad-p = 0.0002. TQ: wild-type 58.40 ± 10.82, HTZ 52.10 ± 8.91, HMZ 60.21 ± 11.55. Ad -: wild-type 19.14 ± 8.06, HTZ 9.18 ± 2.53, HMZ 15.73 ± 5.52. Ad +, wild-type 16.89 ± 9.84, HTZ 18.61 ± 4.52, HMZ 9.30 ± 2.72. OP: wild-type 5.56 ± 1.96, HTZ 20.10 ± 7.08, HMZ 14.75 ± 4.75. Control, n = 10; HTZ, n = 11; HMZ, n = 9. *p < 0.05, **p < 0.01, ***p < 0.001, ****p < 0.0001. Data are represented as mean ± SEM.

It has been reported that Nlgn1 KO mice present decreased spatial memory in the Morris water maze.[16] To analyze if spatial memory was affected in Nlgn1 Thr271fs mice we used the Barnes maze test, a less stressful test for terrestrial rodents than an aquatic maze.[34] During training, mice learn to find shelter in one hole located at the periphery using spatial cues located in the proximity. The latency to find the escape hole decreased in HTZ and HMZ Nlgn1 Thr271fs mice during the training sessions, indicating normal learning, and showed a shorter latency on the third day for HTZ Nlgn1 Thr271fs mice (Figure 2B). On the evaluation of the spatial memory at one day after training, HTZ and HMZ Nlgn1 Thr271fs mice showed clear preference for the target quadrant, similar to wild-type mice (Figure 2B). Therefore, spatial memory was not found affected in Nlgn1 Thr271fs adult mice.

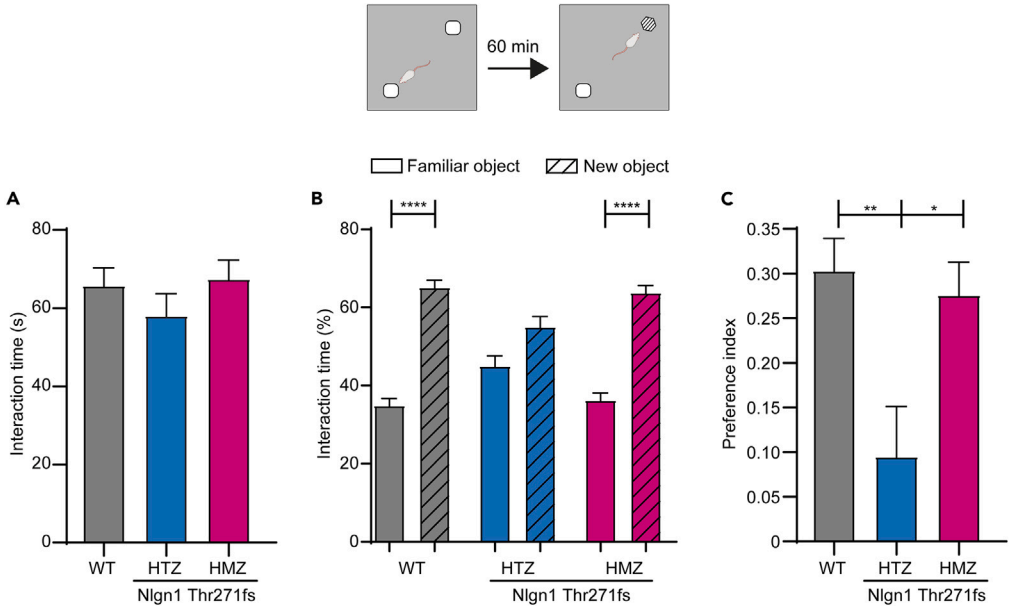

Figure 3. Altered recognition memory in HTZ Nlgn1 Thr271fs mice

(A) Total interaction time (s) during exploration (one-way ANOVA with Tukey's post-hoc analysis. $F_{(2.43)} = 0.3897$, $p = 0.389$. Wild-type, 65.63 ± 4.67; HTZ, 58.02 ± 5.62; HMZ, 67.37 ± 4.90).

(B) Interaction time (%) with the familiar or novel object 1 h after exploration. Differences in interaction time with new and familiar object within each genotype (wild-type, familiar vs. novel object paired t-test $p < 0.0001$; HTZ, familiar vs. novel object paired t-test $p = 0.0778$; HMZ, familiar vs. novel object paired t-test $p < 0.0001$. Wild-type, familiar 34.87 ± 1.83, novel 65.13 ± 1.83; HTZ, familiar 44.97 ± 2.68, novel 55.03 ± 2.68; HMZ, familiar 36.23 ± 1.87, novel 63.77 ± 1.87. Corresponding time in s: Wild-type, familiar 17.69 ± 1.20, novel 34.04 ± 2.81; HTZ, familiar 23.70 ± 2.73, novel 27.97 ± 3.12; HMZ, familiar 25.55 ± 2.62, novel 44.03 ± 4.18).

(C) Preference index (one-way ANOVA with Tukey's post-hoc analysis. $F_{(2.44)} = 6.32$, $p = 0.0039$, wild-type vs. HTZ $p = 0.0063$, wild-type vs. HMZ $p = 0.9114$, HTZ vs. HMZ $p = 0.0195$. Wild-type, 0.30 ± 0.03; HTZ, 0.09 ± 0.05; HMZ, 0.27 ± 0.03). Wild-type, n = 15; HTZ, n = 17; HMZ, n = 15. *$p < 0.05$, **$p < 0.01$, ****$p < 0.0001$. Data are represented as mean ± SEM. See also Figure S3.

Impaired consolidation of recognition memory in heterozygous, but not homozygous, Nlgn1 Thr271fs mice

Recognition memory depends on the ability to distinguish novelty from familiarity and the difficulty in recognizing familial stimuli is one of the early traits of cognitive decline observed in AD. In rodents, recognition memory can be evaluated in the novel object recognition test, which relies on the innate preference of rodents for a novel object presented along with a familiar one. Surprisingly, we found that HTZ Nlgn1 Thr271fs mice showed impaired recognition memory, which was not shared by HMZ Nlgn1 Thr271fs mice (Figures 3A–3C). During the initial presentation to the two copies of the object, Nlgn1 Thr27fs and wild-type mice showed similar interaction time, indicating normal exploration (Figure 3A). One hour later, mice were exposed to a copy of the previously exposed object, the familiar object, and to a new object of similar size. Wild-type and HMZ Nlgn1 mice showed preferential interaction with the novel object (Figures 3B and 3C). However, HTZ Nlgn1 Thr271fs mice exhibited similar interaction time with the novel and familiar objects, indicating a lack of novelty discrimination (Figures 3B and 3C). Expression of recognition memory depends on an encoding, a consolidation and a retrieval phase.[35,36] To determine if the initial encoding of recognition memory or the subsequent consolidation step were responsible for the impaired recognition memory of the HTZ Nlgn1 Thr271fs mice, we analyzed object recognition memory at different delays after object presentation. Notably, HTZ Nlgn1 Thr271fs mice exhibited preferential interaction with the novel object when recognition memory was explored 5 min after object presentation (Figure 4A). These data showed that HTZ Nlgn1 Thr271fs mice are able to distinguish novelty from familiarity at short delays, indicating normal encoding. The consolidation phase is formed at an early time after object presentation.[35,36] Remarkably, the preferential interaction of HTZ Nlgn1 Thr271fs mice with the novel object decreased at 15-min delay and it was lost at 30 min after object presentation (Figures 4B

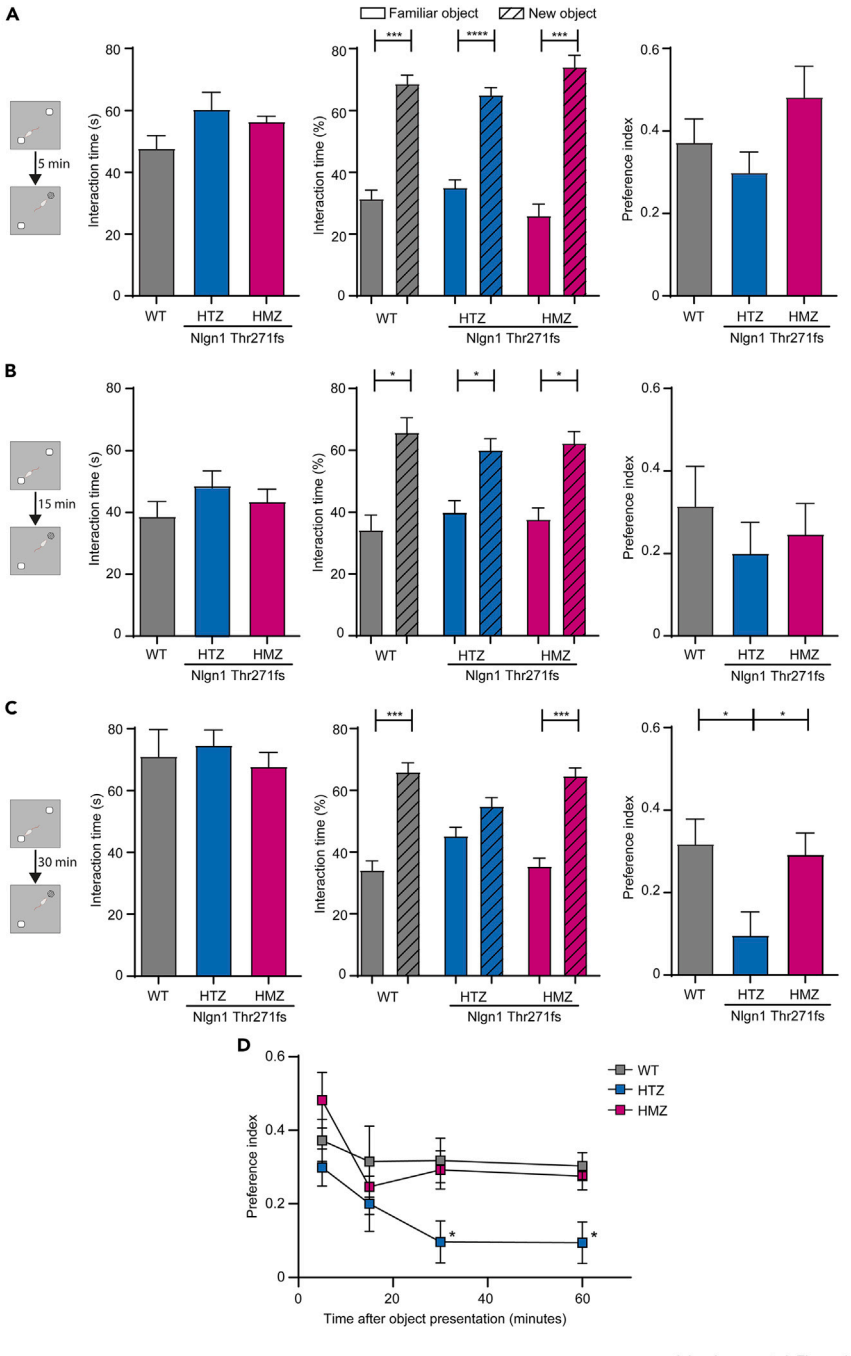

Figure 4. Impaired consolidation of recognition memory in HTZ Nlgn1 Thr271fs mice

(A) Recognition memory at 5 min after exploration. Interaction time (s) during exploration (left) (one-way ANOVA analysis. $F_{(2.31)} = 1.688$, p = 0.201. Wild-type, 47.65 ± 4.21; HTZ, 60.31 ± 5.52; HMZ, 56.30 ± 1.86. Interaction time (%) with familiar or novel objects (center). Differences in interaction time with new and familiar object within each genotype (wild-type, familiar vs. novel object paired t-test p = 0.0001; HTZ, familiar vs. novel object paired t-test p < 0.0001; HMZ familiar vs. novel object paired t-test p = 0.0004. Wild-type, familiar 31.40 ± 2.86, novel 68.60 ± 2.86; HTZ, familiar 35.06 ± 2.51, novel 64.94 ± 2.51; HMZ, familiar 25.92 ± 3.78, novel 74.08 ± 3.78. Corresponding time in s: Wild-type, familiar 13.05 ± 2.21, novel 28.60 ± 4.21; HTZ, familiar 15.84 ± 2.09, novel 28.75 ± 2.76; HMZ, familiar 11.78 ± 2.13, novel 34.08 ± 6.33). Preference index (right) (one-way ANOVA analysis. $F_{(2.31)} = 2.269$, p = 0.120. Wild-type, 0.37 ± 0.05; HTZ, 0.29 ± 0.05; HMZ, 0.48 ± 0.07). Wild-type, n = 10; HTZ, n = 16; HMZ, n = 8.

Figure 4. *Continued*

(B) Recognition memory at 15 min after exploration. Interaction time (s) during exploration (left) (one-way ANOVA analysis. $F_{(2.26)}$ = 1.180, p = 0.323. Wild-type, 38.65 ± 4.84; HTZ, 48.59 ± 4.79; HMZ, 43.46 ± 4.06). Interaction time (%) with familiar or novel objects (center). Differences in interaction time with new and familiar object within each genotype (wild-type, familiar vs. novel object paired t-test p = 0.011; HTZ, familiar vs. novel object paired t-test p = 0.021; HMZ familiar vs. novel object paired t-test p = 0.013.Wild-type, familiar 34.26 ± 4.82, novel 65.74 ± 4.82; HTZ, familiar 39.98 ± 3.75, novel 60.06 ± 3.75; HMZ, familiar 37.68 ± 3.75, novel 62.32 ± 3.75. Corresponding time in s: Wild-type, familiar 12.74 ± 2.08, novel 26.11 ± 3.59; HTZ, familiar 16.82 ± 2.17, novel 25.34 ± 3.13; HMZ, familiar 15.49 ± 2.34, novel 25.32 ± 2.46). Preference index (right) (one-way ANOVA analysis. $F_{(2.26)}$ = 0.507, p = 0.607. Wild-type, 0.31 ± 0.09; HTZ, 0.20 ± 0.07; HMZ, 0.24 ± 0.07). Wild-type, n = 9; HTZ, n = 12; HMZ, n = 8.

(C) Recognition memory at 30 min after exploration. Interaction time (s) during exploration (left) (one-way ANOVA analysis. $F_{(2.29)}$ = 0.331, p = 0.720. Wild-type, 71.03 ± 8.65; HTZ, 74.58 ± 4.98; HMZ, 67.74 ± 4.59). Interaction time (%) with familiar or novel objects (center). Differences in interaction time with new and familiar object within each genotype (wild-type, familiar vs. novel object paired t-test p = 0.0008; HTZ, familiar vs. novel object paired t-test p = 0.114; HMZ, familiar vs. novel object paired t-test p = 0.0005. Wild-type, familiar 34.12 ± 3.03, novel 65.88 ± 3.03; HTZ, familiar 45.19 ± 2.84, novel 54.81 ± 2.84; HMZ, familiar 35.40 ± 2.61, novel 64.60 ± 2.61. Corresponding time in s: Wild-type, familiar 20.46 ± 2.28, novel 40.25 ± 4.67; HTZ, familiar 29.36 ± 3.38, novel 35.63 ± 4.66; HMZ, familiar 21.89 ± 1.56, novel 43.51 ± 7.04). Preference index (right) (one-way ANOVA with Holm-Sidak's post-hoc analysis. $F_{(2.29)}$ = 4.77, p = 0.016, wild-type vs. HTZ p = 0.032, wild-type vs. HMZ p = 0.778, HTZ vs. HMZ p = 0.044. Wild-type, 0.31 ± 0.06; HTZ, 0.09 ± 0.05; HMZ, 0.29 ± 0.05). Wild-type, n = 9; HTZ, n = 14; HMZ, n = 9.

(D) Graphical representation showing the preference index at different delays after object presentation (mixed-effects model with Tukey's post-hoc analysis. F(2. 53) = 7.367, p = 0.0015. P-values< 0.05: 30 min: WT vs. HTZ p = 0.0391; HTZ vs. HMZ p = 0.0488. 60 min: WT vs. HTZ p = 0.012; HTZ vs. HMZ p = 0.033). *p < 0.05, ***p < 0.001, ****p < 0.0001. Data are represented as mean ± SEM. See also Figure S3.

and 4C). These defects in the consolidation of recognition memory were found specific for HTZ Nlgn1 Thr271fs mice, as total loss of Nlgn1 expression in HMZ Nlgn1 Thr271fs mice did not affect recognition memory at these intervals (Figures 4B and 4C). These data indicate that a partial loss of Nlgn1 produces a delay-dependent amnesia for recognition memory in mice.

Permanence of specific memory deficits in old heterozygous Nlgn1 Thr271fs mice

The behavioral analysis identified deficits in recognition memory specific to HTZ Nlgn1 Thr271fs mice. To rule out a later convergence of HTZ Nlgn1 Thr271fs mice to the memory deficits found in HMZ Nlgn1 Thr271fs mice we performed behavioral analysis in old HTZ Nlgn1 Thr271fs mice. For that, we grew independent cohorts of HTZ Nlgn1 Thr271fs mice up to 15–18 months. In the fear-conditioning test, old HTZ Nlgn1 Thr271fs mice showed normal conditioning and freezing response, compared with wild-type mice (Figure S3A). However, recognition memory was impaired in old HTZ Nlgn1 Thr271fs mice (Figure S3B), as it was found in young adult HTZ Nlgn1 Thr271fs mice. Analysis at different times after object presentation confirmed a delay-dependent impairment in recognition memory in HTZ Nlgn1 Thr271fs mice at an old age (Figures S3C–S3E). Therefore, the lack of acquisition of fear-memory impairments together with the permanence of recognition memory deficits in old HTZ Nlgn1 Thr271fs mice indicated that a partial loss of Nlgn1 impacts memory in a specific manner that cannot be accelerated by a full inhibition of Nlgn1.

Hippocampal LTP is preserved in heterozygous, but decreased in homozygous, Nlgn1 Thr271fs mice at a young adult age

The behavioral characterization of Nlgn1 Thr271fs mice showing a differential effect on memory for the HTZ or the HMZ mutation suggested a distinct synaptic mechanism for a partial or total loss of Nlgn1. The hippocampus is involved in spatial and non-spatial memory[37,38] and synapses formed by CA3 and CA1 neurons are arguably the best-studied synapses in the scientific literature. Moreover, it has been previously reported that LTP at CA3-CA1 synapses is decreased in Nlgn1 KO mice suggesting that these synapses are sensitive to changes in Nlgn1 levels.[16] We performed extracellular Field excitatory postsynaptic potential (fEPSP) recordings in the CA1 region of acute hippocampal slices from Nlgn1 Thr271fs mice at a young adult age (4–6 months). Input-output curves were found normal at CA3-CA1 synapses of young adult Nlgn1 Thr271fs mice either harboring the mutation at heterozygosis or homozygosis (Figures 5A and 5B). Similarly, paired-pulse facilitation (PPF) was not altered in HTZ or HMZ Nlgn1 Thr271fs mice at a young adult age (Figure 5C). These data indicated that a partial or total loss of Nlgn1 does not affect basal synaptic transmission or presynaptic plasticity in young adult mice. Then, we analyzed LTP at CA3-CA1 synapses. High-frequency stimulation (HFS) at Schaffer collaterals induced an increase in synaptic efficacy at CA1 synapses of wild-type mice that last for the 120 min of the recording session (Figures 5D–5F). The LTP in HTZ

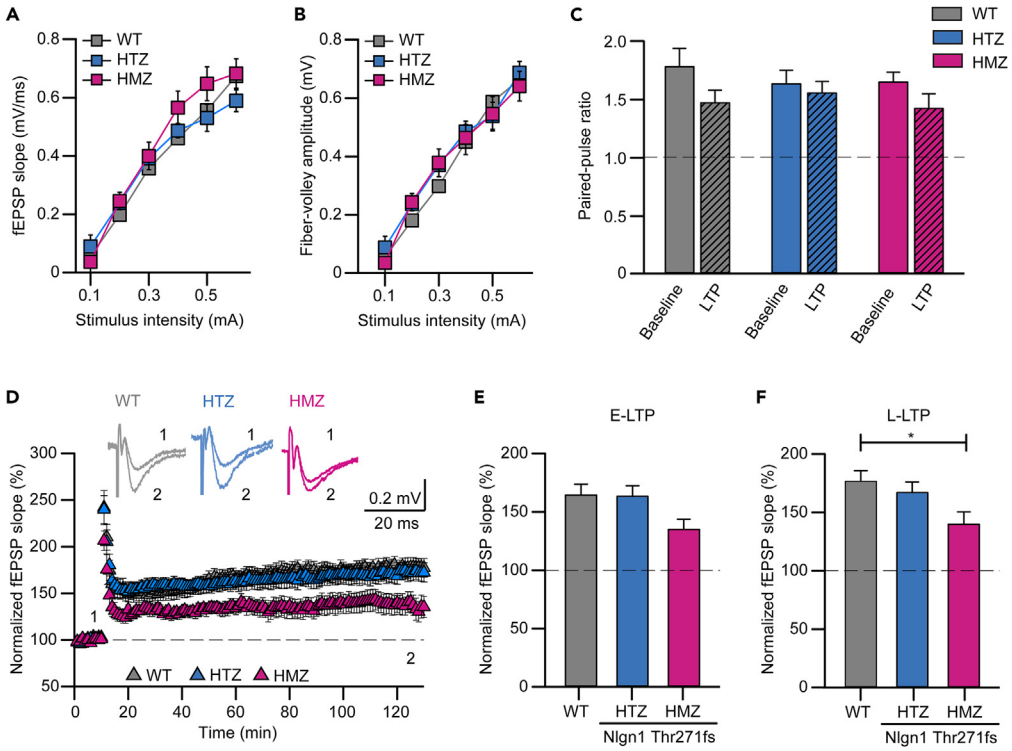

Figure 5. Normal basal synaptic transmission and LTP in CA1 neurons of young adult Nlgn1 Thr271fs mice

(A and B) Input-output curves. Averaged fEPSP slope (two-way repeated measures ANOVA analysis. $F_{(2,15)} = 2.119$, $p = 0.171$) (A) and fiber-volley amplitude (two-way repeated measures ANOVA analysis. $F_{(2, 15)} = 0.072$, $p = 0.930$) (B) plotted against stimulus intensity. Wild-type, n = 6; HTZ, n = 6; HMZ, n = 6.

(C) paired-pulse ratio (PPR) in acute hippocampal slices of young adult mice (unpaired t-test, wild-type: baseline vs. LTP $p = 0.117$. HTZ: baseline vs. LTP $p = 0.613$. HMZ: baseline vs. LTP $p = 0.163$). Wild-type, n = 12; HTZ, n = 19; HMZ, n = 7.

(D) Time course of averaged fEPSP slope before and after LTP induction in the hippocampal CA1 region. Inset, representative traces.

(E and F) Quantitation of E-LTP (E) and L-LTP (F) (one-way ANOVA with Holm-Sidak's post-hoc analysis. E-LTP: $F_{(2,42)} = 1.887$, $p = 0.164$. L-LT: $F_{(2,42)} = 3.255$, $p = 0.049$, wild-type vs. HTZ $p = 0.610$, wild-type vs. HMZ $p = 0.046$, HTZ vs. HMZ $p = 0.067$). Wild-type, n = 15; HTZ, n = 22; HMZ, n = 8. *$p < 0.05$. Data are represented as mean ± SEM.

Nlgn1 Thr271fs mice was found of similar magnitude to that of wild-type mice (Figures 5D–5F). However, LTP was decreased in HMZ Nlgn1 Thr271fs mice (Figures 5D–5F), in accordance with the impaired LTP reported in Nlgn1 KO mice.[16] These data indicated that a total loss of Nlgn1 produced LTP deficits in CA1 hippocampal neurons, which are not expressed by a partial loss of Nlgn1 in young adult mice.

Decreased synaptic transmission and LTP in the hippocampus of heterozygous Nlgn1 Thr271fs mice during aging

Aging is the most relevant non-genetic factor associated with AD. Even in the face of causative mutations in FAD-linked genes, the pathogenic mechanisms are thought to progress during a relatively prolonged time period.[4] Therefore, we decided to explore if the synaptic function of Nlgn1 Thr271fs mice was altered during aging (Figure 6). In a first set of experiments, we performed fEPSP recordings in hippocampal CA3-CA1 synapses of 12-months old mice. In HMZ Nlgn1 Thr271fs mice, input-output curves (Figures 6A and 6B) and PPF recordings (Figure 6C) were normal. LTP in 12-months-old HMZ Nlgn1 Thr271fs mice was decreased at a similar extent than at a younger age (Figures 6D–6F), indicating that the deficits in hippocampal plasticity associated with a total loss of Nlgn1 do not aggravate during this time period. Strikingly, a different situation was found in HTZ Nlgn1 Thr271fs mice. In contrast to the results obtained at a younger age, input-output curves were specifically decreased in 12-months old HTZ Nlgn1 Thr271fs mice compared with both wild-type and HMZ Nlgn1 Thr271fs mice (Figures 6A and 6B). PPF was not altered in HTZ Nlgn1 Thr271fs mice (Figure 6C), indicating normal release probability. Importantly, LTP decreased in

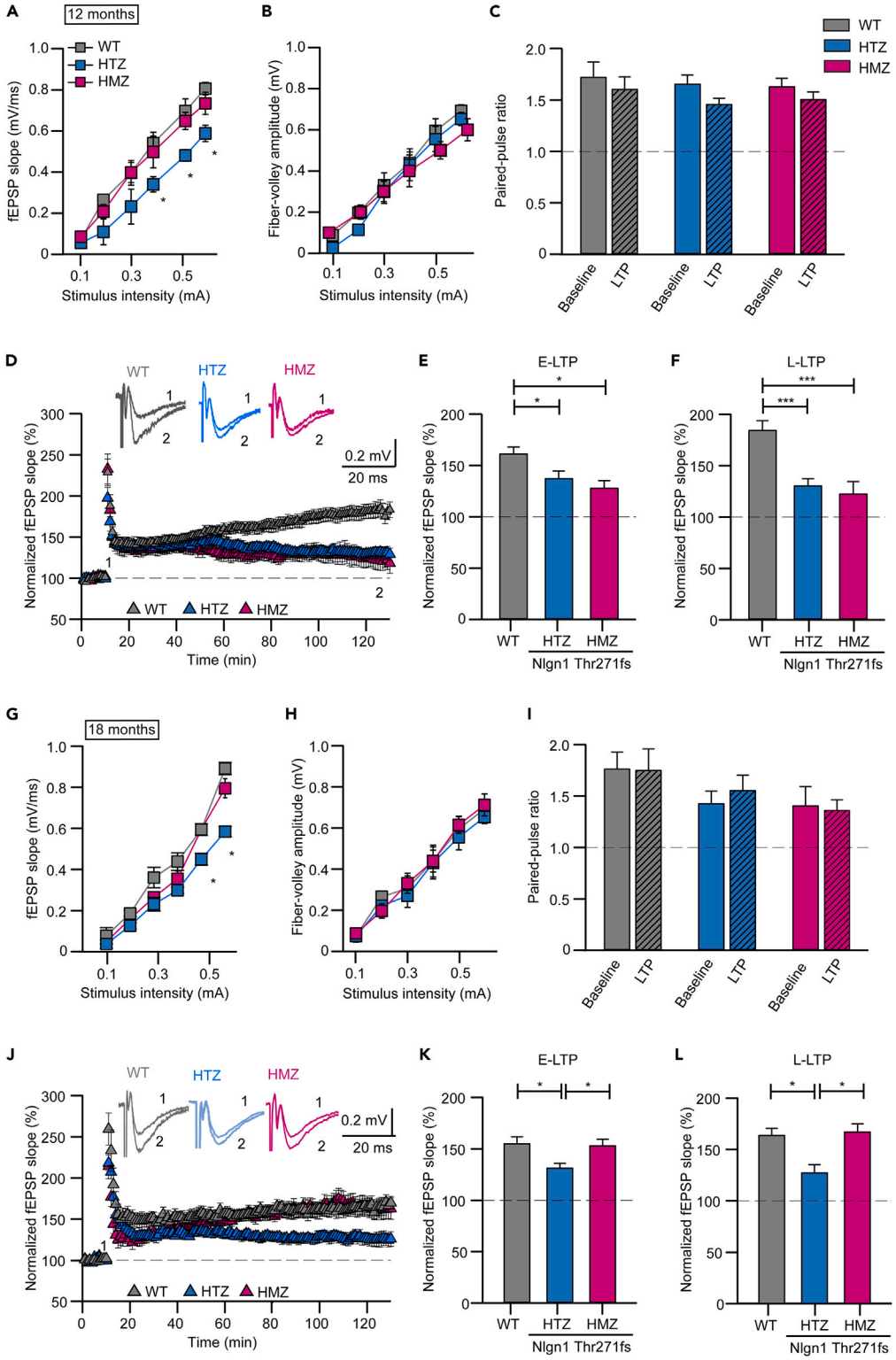

Figure 6. Impaired basal synaptic transmission and LTP in hippocampal CA1 neurons of aged Nlgn1 Thr271fs mice

(A and B) Input-output curves. Averaged fEPSP slope (two-way repeated measures ANOVA with Tukey's post-hoc analysis. $F_{(2, 15)} = 3.616$, p = 0.048, wild-type vs. HTZ: p = 0.576, p = 0.068, p = 0.147, p = 0.032, p = 0.025, p = 0.011) (A) and

Figure 6. *Continued*

fiber-volley amplitude (two-way repeated measures ANOVA analysis $F_{(2, 15)} = 0.062$, $p = 0.940$) (B) plotted against stimulus intensity in 12-months old mice. Wild-type, n = 6; HTZ, n = 6; HMZ, n = 6.

(C) PPR in the CA1 region of the hippocampus of 12 months mice (unpaired t-test, wild-type: baseline vs. LTP $p = 0.517$; HTZ: baseline vs. LTP $p = 0.075$; HMZ baseline vs. LTP $p = 0.285$). Wild-type, n = 18; HTZ, n = 15; HMZ, n = 8.

(D) Averaged fEPSP slope before and after LTP induction in CA1 region at 12 months. Inset, representative traces. Wild-type, n = 22; HTZ, n = 18; HMZ, n = 12.

(E and F) Quantitation of E-LTP (E) and L-LTP (F) at 12 months (one-way ANOVA with Holm-Sidak's post-hoc analysis. E-LTP: $F_{(2,49)} = 5.445$, $p = 0.007$, wild-type vs. HTZ $p = 0.037$, wild-type vs. HMZ $p = 0.012$, HTZ vs. HMZ $p = 0.410$; L-LTP: $F_{(2,49)} = 13.08$, $p < 0.001$, wild-type vs. HTZ $p < 0.001$, wild-type vs. HMZ $p < 0.001$, HTZ vs. HMZ $p = 0.599$).

(G and H) Input-output curves at 18 months. Averaged fEPSP slope (two-way repeated measures ANOVA with Tukey's post-hoc analysis. $F_{(2, 15)} = 9.488$, $p = 0.005$, wild-type vs. HTZ $p = 0.397$, $p = 0.20$, $p = 0.055$, $p = 0.098$, $p = 0.045$, $p = 0.015$) (G) and fiber-volley amplitude (two-way repeated measures ANOVA analysis, $F_{(2,15)} = 0.725$, $p = 0.501$) (H) plotted against stimulus intensity in 18-month mice. Wild-type, n = 6; HTZ, n = 6; HMZ, n = 6.

(I) PPR at 18 months (unpaired t-test, wild-type: baseline vs. LTP $p = 0.957$; HTZ: baseline vs. LTP $p = 0.526$; HMZ: baseline vs. LTP $p = 0.848$). Wild-type, n = 6; HTZ, n = 7; HMZ, n = 6.

(J) fEPSP before and after LTP induction in the hippocampal CA1 region of 18-months old mice. Inset, representative traces. Wild-type, n = 7; HTZ, n = 8; HMZ, n = 8.

(K and L) Quantitation of E-LTP (K) and L-LTP (L) at 18 months (one-way ANOVA with Holm-Sidak's post-hoc analysis. E-LTP: $F_{(2,20)} = 4.781$, $p = 0.020$, wild-type vs. HTZ $p = 0.038$, wild-type vs. HMZ $p = 0.821$, HTZ vs. HMZ $p = 0.035$; L-LTP: $F_{(2,20)} = 5.809$, $p = 0.010$, wild-type vs. HTZ $p = 0.025$, wild-type vs. HMZ $p = 0.805$, HTZ vs. HMZ $p = 0.017$). *$p < 0.05$, ***$p < 0.001$. Data are represented as mean ± SEM.

12-months old HTZ Nlgn1 Thr271fs mice at a similar level found for the HMZ mutation, but differing from normal LTP in younger HTZ mice (Figures 6D–6F). These data indicated that a partial loss of Nlgn1 resulted in age-dependent deficits in synaptic transmission and plasticity in CA1 hippocampal neurons of HTZ Nlgn1 Thr271fs mice.

To further analyze the effect of aging we performed fEPSP recordings in CA3-CA1 synapses at 18 months. Again, we found a significant decrease in the input-output responses of HTZ Nlgn1 Thr271fs mice at 18 months, which was not detected in HMZ Nlgn1 Thr271fs mice of the same age (Figures 6G and 6H). PPF was not altered in HTZ Nlgn1 Thr271fs mice at 18 months (Figure 6I). Moreover, LTP at CA3-CA1 synapses of HTZ Nlgn1 Thr271fs mice was decreased at 18 months at similar levels as those found at 12 months (Figures 6J–6L). In contrast, LTP in HMZ Nlgn1 Thr271fs mice was of similar magnitude than in wild-type mice of the same age (Figures 6J–6L). These data indicated that a partial loss of Nlgn1 produced permanent age-dependent deficits in glutamatergic synaptic transmission and plasticity in the hippocampus, which are not observed in young adult individuals.

Age-dependent loss of AMPAR response in heterozygous Nlgn1 Thr271fs mice

Synapse loss is a main clinical finding associated with AD. The age-dependent decrease in basal synaptic transmission of hippocampal CA1 neurons in HTZ Nlgn1 Thr271fs mice suggested that a partial loss of Nlgn1 produces a decrease in the number or in the function of synapses during aging. Compared with wild-type mice, the density of dendritic spines was found similar in Golgi-Cox staining of CA1 neurons of adult and old HTZ Nlgn1 Thr271fs mice (Figure 7A). Furthermore, neuronal density was not affected in HTZ Nlgn1 Thr271fs mice (Figure S4). These data suggested that a mechanism other than a decrease in the number of morphological synapses is associated with a partial loss of Nlgn1. Decreased NMDAR response is a common feature associated with a total loss of Nlgn1 in young mice, although the effects produced by a chronic and partial loss of Nlgn1 on NMDAR- and AMPAR-responses are not known. To address this question, we performed patch-clamp recordings in CA1 hippocampal neurons of HTZ Nlgn1 Thr271fs mice. In juvenile mice (1–2 months), the AMPAR- and NMDAR-currents of HTZ Nlgn1 Thr271fs mice were normal as compared with wild-type mice (Figure 7B). Accordingly, NMDA/AMPA ratio was not altered at this age (Figure 7C). Furthermore, recordings of excitatory postsynaptic currents (EPSCs) at −70 mV holding potential showed normal input-output responses in HTZ Nlgn1 Thr271fs mice, in agreement with normal AMPAR synaptic response at this young age (Figure 7D). Then, we measured NMDAR- and AMPAR-currents in hippocampal CA1 neurons in old mice (18 months), when basal synaptic transmission and LTP were decreased in HTZ Nlgn1 Thr271fs mice (Figure 6). Interestingly, AMPAR-mediated synaptic transmission was specifically reduced in CA1 hippocampal neurons of old HTZ Nlgn1 Thr271fs mice, but NMDAR-dependent currents were found normal (Figure 7E). As a consequence, NMDA/AMPA ratio was increased in old HTZ Nlgn1 Thr271fs mice (Figure 7F). Input-output experiments performed at −70 mV

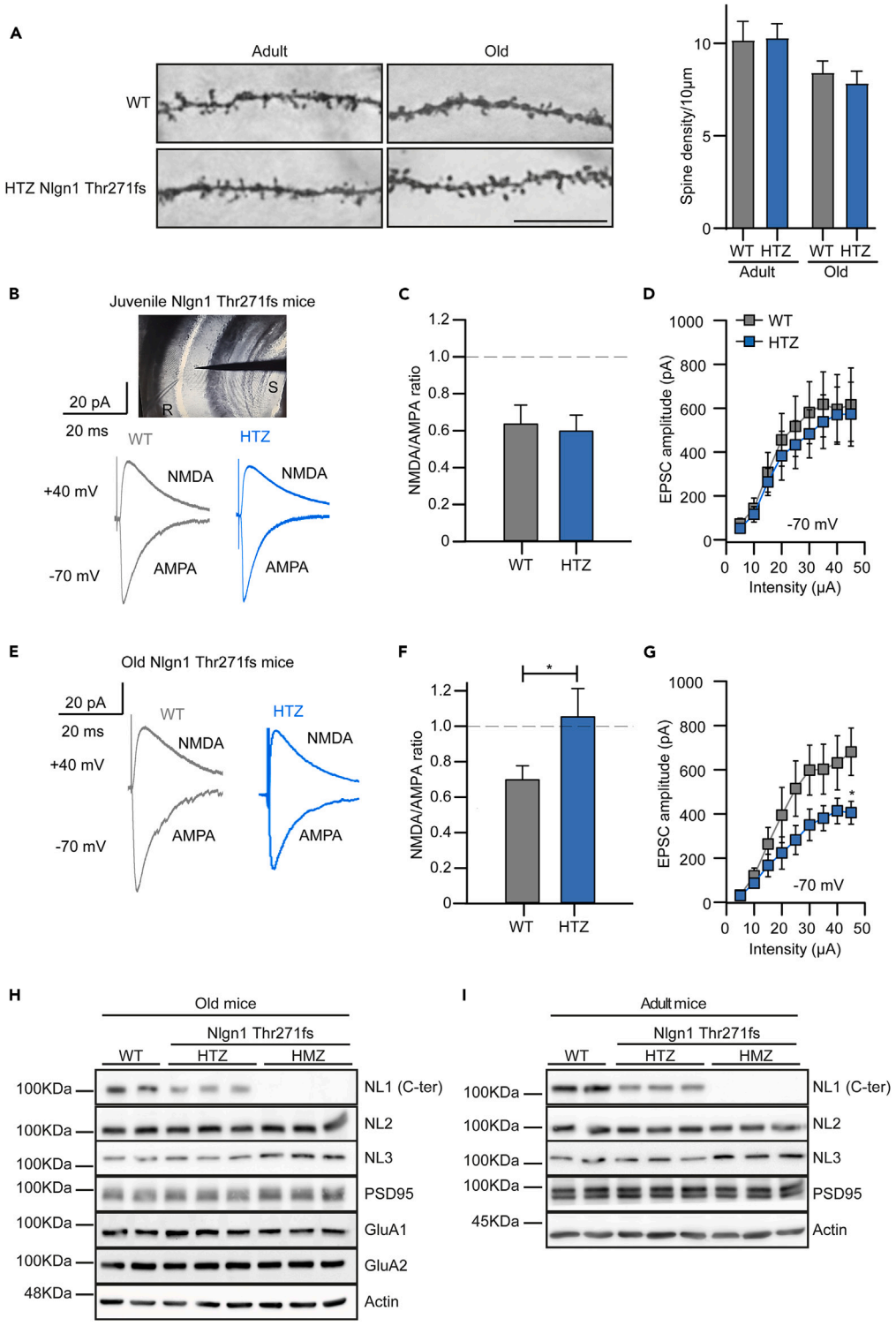

Figure 7. Age-dependent loss of AMPAR response in HTZ Nlgn1 Thr271fs mice

(A) Normal dendritic spine density in HTZ Nlgn1 Thr271fs mice. Representative Golgi-Cox images and quantitation of dendritic spines density in CA1 neurons of the hippocampus of adult (5–6 months) and old (24 months) mice are shown (adult: wild-type vs. HTZ unpaired t-test p = 0.921; old: wild-type vs. HTZ unpaired t-test p = 0.543. Adult mice: wild-type, 10.16 ± 1.03; HTZ, 10.29 ± 0.77. Old mice: wild-type, 8.41 ± 0.62; HTZ, 7.84 ± 0.65). Four to five independent animals per condition, 8–20 dendritic segments per animal.

Figure 7. *Continued*

(B) Whole-cell voltage-clamp experiments in hippocampal CA1 neurons from wild-type and HTZ Nlg1 Thr271fs mice at 1–2 months. AMPAR and NMDAR EPSCs were recorded at −70 and +40 mV, respectively.

(C) Normal NMDAR/AMPAR ratio in HTZ Nlgn1 Thr271fs mice at 1–2 months (unpaired t-test p = 0.784). Wild-type, n = 12; HTZ, n = 11.

(D) Input-output curves in hippocampal CA1 neurons from 1 to 2 months old mice recorded in whole-cell voltage-clamp experiments at −70 mV holding potential (multiple unpaired t-test p = 0.569, p = 0.902, p = 0.836, p = 0.398, p = 0.672, p = 0.648, p = 0.982, p = 0.850, p = 0.757). Wild-type, n = 10; HTZ, n = 7.

(E) Representative traces of AMPAR and NMDAR EPSCs recorded in 18-months old CA1 hippocampal neurons. AMPAR EPSC was selectively reduced in HTZ Nlg1 Thr271fs mice.

(F) Increased NMDAR/AMPAR ratio in HTZ Nlgn1 Thr271fs mice at 18 months (unpaired T-test p = 0.045). Wild-type, n = 12; HTZ, n = 11.

(G) Decreased Input-output currents in 18-months old HTZ Nlgn1 Thr271fs mice recorded in EPSC experiments at −70 mV (multiple unpaired t-test p = 0.069, p = 0.425, p = 0.289, p = 0.242, p = 0.112, p = 0.078, p = 0.090, p = 0.117, p = 0.032). Wild-type, n = 7; HTZ, n = 8.

(H and I) Expression of synaptic components in the hippocampus of Nlgn1 Thr271fs mice in 12-months old (H) and 6-months old (I) individuals. ((H) Nlgn1, one-way ANOVA with Tukey's post-hoc analysis. $F_{(2.6)}$ = 251.6, p < 0.0001, wild-type vs. HTZ p < 0.0001, wild-type vs. HMZ p < 0.0001, HTZ vs. HMZ p < 0.0001. Wild-type, 1 ± 0.04; HTZ, 0.517 ± 0.035; HMZ: 0.005 ± 0.002. Nlgn2, one-way ANOVA. $F_{(2.6)}$ = 0.199, p = 0.825. Wild-type 1 ± 0.061; HTZ 1.078 ± 0.060; HMZ 1.122 ± 0.0531. Nlgn3, one-way ANOVA with Holm-Sidak's post-hoc analysis. $F_{(2.6)}$ = 287.2, p < 0.0001, wild-type vs. HTZ p = 0.208, wild-type vs. HMZ p = 0.0005, HTZ vs. HMZ p = 0.002. Wild-type 1 ± 0.09; HTZ 1.28 ± 0.10; HMZ 2.196 ± 0.107. PSD95, one-way ANOVA. $F_{(2.6)}$ = 0.44, p = 0.662. Wild-type 1 ± 0.085; HTZ 1.090 ± 0.136; HMZ 1.14 ± 0.047. GluA1, one-way ANOVA. $F_{(2.6)}$ = 2.76, p = 0.15. Wild-type 1 ± 0.06; HTZ 1.051 ± 0.09; HMZ 0.835 ± 0.027. GluA2, one-way ANOVA. $F_{(2.6)}$ = 0.068, p = 0.934. Wild-type 1 ± 0.15; HTZ 1.03 ± 0.046; HMZ 1.041 ± 0.044. (I) Nlgn1, one-way ANOVA with Tukey's post-hoc analysis. $F_{(2.6)}$ = 105.2, p < 0.0001, wild-type vs. HTZ p = 0.006, wild-type vs. HMZ p < 0.0001, HTZ vs. HMZ p = 0.0012. Wild-type 1 ± 0.08; HTZ 0.468 ± 0.007; HMZ 0.001 ± 0.0010. Nlgn2, one-way ANOVA. $F_{(2.6)}$ = 0.37, p = 0.702. Wild-type 1 ± 0.03; HTZ 0.952 ± 0.091; HMZ 0.922 ± 0.051. Nlgn3, one-way ANOVA with Holm-Sidak's post-hoc analysis. $F_{(2.6)}$ = 13.53, p = 0.0096, wild-type vs. HTZ p = 0.47, wild-type vs. HMZ p = 0.0177, HTZ vs. HMZ p = 0.0177. Wild-type 1 ± 0.20; HTZ 1.16 ± 0.10; HMZ 1.952 ± 0.13. PSD95, one-way ANOVA. $F_{(2.6)}$ = 0.091, p = 0.914. Wild-type 1 ± 0.059; HTZ 1.037 ± 0.082; HMZ 1.012 ± 0.032). The expression of Nlgn1, Nlgn2, Nlgn3, PSD95, GluA1 and GluA2 was analyzed with specific antibodies, as indicated. Scale bar, 10 μm *p < 0.05. Data are represented as mean ± SEM. See also Figure S4.

holding potentials in parallel EPSCs recordings confirmed the decrease in AMPAR-synaptic transmission in CA1 hippocampal neurons of old HTZ Nlgn1 Thr271fs mice (Figure 7G). These data indicated an age-dependent decrease in AMPAR-mediated synaptic transmission upon a partial loss of Nlgn1.

The reduction in AMPAR-mediated synaptic response of HTZ Nlgn1 Thr271fs mice was not associated with changes in the hippocampal levels of GluA1 or GluA2 subunits of the AMPAR (Figure 7H). It has been reported that loss of Nlgn1 expression produces a compensatory increase in Nlgn3 levels in Nlgn1 KO mice.[16,29] Since Nlgn3 regulates AMPAR responses in hippocampal CA1 neurons,[39,40] we wondered if changes in Nlgn3 could account for the reduced AMPAR-currents in old HTZ Nlgn1 Thr271fs mice. However, Nlgn3 levels were found normal in the hippocampus of young and old HTZ Nlgn1 Thr271fs mice (Figures 7H and 7I), indicating a direct role of reduced Nlgn1 expression in the decrease of AMPAR-synaptic transmission. In contrast, hippocampal Nlgn3 selectively increased 2-fold in HMZ Nlgn1 Thr271fs mice in adult and old individuals (Figures 7H and 7I). Nlgn2 levels did not change in the different conditions (Figures 7H and 7I). These results point at the expression of a synaptic mechanism that can partly compensate the absence of Nlgn1, which is not triggered upon a partial loss of Nlgn1. Together, these data indicate that the partial loss of Nlgn1 in HTZ Nlgn1 Thr271fs mice produces an age-dependent and selective decrease in AMPAR-mediated synaptic transmission that leads to a loss of functional synapses.

DISCUSSION

Nlgn1 is a postsynaptic plasma membrane protein important for glutamatergic synapse function that has been found decreased in AD. In this study, we have generated a mouse model that reproduces a frameshift mutation in the *NLGN1* gene previously identified in heterozygosis in AD.[30] We show that the Nlgn1 Thr271fs mutation abolishes the expression of the Nlgn1 protein in mouse brain, resulting in a partial or null Nlgn1 expression in HTZ or HMZ Nlgn1 Thr271fs mice, respectively. Behavioral characterization of HTZ Nlgn1 Thr271fs mice, which mimics the AD-associated mutation, showed temporally graded antero-grade amnesia for recognition memory. Electrophysiological recordings in CA1 hippocampal neurons of HTZ Nlgn1 Thr271fs mice identified age-dependent decrease in glutamatergic synaptic transmission

and in LTP associated with a reduction in AMPAR-currents. By contrast, HMZ Nlgn1 Thr271fs mice lacking expression of Nlgn1 showed distinct synaptic and behavioral defects, including associative memory. These data show that the AD-related HTZ Nlgn1 Thr271fs mouse presents short-lived recognition memory and age-dependent loss of AMPAR-mediated synaptic transmission and plasticity, indicating a role for decreased Nlgn1 levels in the memory and synapse loss associated with AD.

The *Nlgn1* Thr271fs mutation is expected to generate a downstream STOP codon that abolishes the expression of the mature Nlgn1 protein and it might result in the production of a C-terminally truncated Nlgn1 fragment. Western-blot experiments confirmed the absence of Nlgn1 expressed by the *Nlgn1* Thr271fs allele in mouse brain. However, the N-terminal Nlgn1 protein fragment was marginally detected in overexposed blots of Nlgn1 Thr271fs mice. RT-PCR analysis confirmed a major decreased in the expression of the mutant Nlgn1 Thr271fs allele compared with the WT allele, as expected for an unstable coding mRNA. In our previous work, Nlgn1 Thr271fs mutant fragments could be readily detected in cultured neurons when expressed from cDNA vectors,[30] further suggesting that the instability of the mRNA transcribed from the Nlgn1 Thr271fs allele explains the virtual absence of the mutant Nlgn1 protein fragment. Whereas a role for the N-terminal Nlgn1 fragment cannot be completely ruled out, our data showed that the AD-associated heterozygous Nlgn1 Thr271fs mutation produces a loss-of-function allele, leading to a 50% reduction of Nlgn1 expression. Interestingly, analysis of human samples has detected a similar 50–60% reduction of Nlgn1 in the hippocampus and cortex of AD and FAD patients.[23,24] Additionally, the partial decrease of Nlgn1 is an early event in animal models of AD that may precede for years the onset of AD symptoms in patients.[24,25,28] These data indicate that an early reduction in Nlgn1, either by genetic or non-genetic mechanisms, might be a common feature associated with AD. In this scenario, the Nlgn1 Thr271fs mouse adds further advantages to understand the implications of Nlgn1 in the broader context of AD. Firstly, the Nlgn1 Thr271fs mouse has construct validity. Secondly, as opposed to other AD-associated approaches that likely affect a number of downstream effectors, the mutational reduction in Nlgn1 does not directly affect the expression of other genes, providing specificity. Thirdly, we characterized the memory and synaptic effects produced by a lifelong reduction in Nlgn1, as the decrease in Nlgn1 acts during a relatively large period of time before the diagnosis of the disease.[25,30] Lastly, by comparing HTZ with HMZ Nlgn1 Thr271fs mice we aimed at uncovering specific defects caused by a partial inhibition of Nlgn1, because most current data on the role of Nlgn1 in memory and synapse function relies on the total or near-total inhibition of Nlgn1 in mouse brain.[11,16–20]

Nlgn1 Thr271fs mice present behavioral deficits typically associated with neurodevelopmental disorders, such as hyperactivity, repetitive behavior, and mild deficits in social interaction but only when the mutation is expressed at homozygosis. Blundell et al. found a similar increase in self-grooming time along with subtle deficits in social interaction in Nlgn1 KO mice.[16] The appearance of neurodevelopmental-associated deficits in HMZ, but not HTZ, Nlgn1 Thr271fs mice suggests that for such deficits to occur Nlgn1 levels must decrease below 50%. Among *NLGN* genes, inactivating mutations in X-linked *NLGN3* and *NLGN4X* genes have been found in male patients of neurodevelopmental disorders, who inherited the mutations from their asymptomatic carrier-mothers. Thus, the presence of an unaffected *NLGN3* or *NLGN4X* allele protects from the onset of neurodevelopmental symptoms, in what it seems to be a parallel situation for the Nlgn1 Thr271fs mutation. Whether carriers of inactivating mutations on *NLGN3* and *NLGN4X* genes present age-dependent memory deficits has not been reported.

Memory loss is a hallmark of cognitive decline in AD. We found that the AD-associated Nlgn1 Thr271fs mouse exhibits memory deficits that depend on the level of Nlgn1 inhibition. Recognition memory allows distinguishing familiarity form novelty and it is a form of memory frequently affected in AD patients. Interestingly, we found that the preference for the novel object was spared in HTZ Nlgn1 Thr271fs mice when a 5-min delay was imposed, but inhibited at longer time intervals. However, recognition memory was not affected in HMZ Nlgn1 Thr271fs at the different delay intervals assayed. Conversely, associative fear-memory was found normal in HTZ Nlgn1 Thr271fs mice, but impaired in HMZ Nlgn1 Thr271fs. The delay-dependent deficits in recognition memory of HTZ Nlgn1 Thr271fs mice correspond to a consolidation phase associated with a normal function of the medial temporal lobe,[35,41] establishing a functional significance for reduced Nlgn1 expression in memory consolidation. Furthermore, the permanence in old HTZ Nlgn1 Thr271fs mice of delay-dependent anterograde amnesia for recognition memory, together with the expression of normal fear-memory, indicated that the HTZ Nlgn1 Thr271fs mutation affects brain function in a specific manner that cannot be anticipated by a total loss of Nlgn1.

The altered mechanisms were studied in CA3-CA1 hippocampal synapses of Nlgn1 Thr271fs mice. Interestingly, we found that a partial reduction of Nlgn1 produces an age-dependent decrease in glutamatergic synaptic transmission and plasticity in the hippocampus. Input-output responses of CA1 hippocampal neurons decreased in middle-aged and old HTZ Nlgn1 Thr271fs mice in parallel to a reduction of hippocampal LTP, although no such impairments were observed in the hippocampus of young adult HTZ Nlgn1 Thr271fs mice. By contrast, HMZ Nlgn1 Thr271fs showed normal input-output responses but decreased hippocampal LTP at a young age. Presynaptic release probability was unaltered in Nlgn1 Thr271fs mice either harboring the mutation at heterozygosis or homozygosis, in agreement with a postsynaptic function of Nlgn1. Therefore, the distinct synaptic defects in HTZ and HMZ Nlgn1 Thr271fs mice could provide an explanation for the associated differences in behavior. The age-dependent loss of AMPAR responses in HTZ Nlgn1 Thr271fs mice indicated by the input-output experiments were further confirmed by EPSCs recordings in CA1 hippocampal neurons, which identified a specific decreased in AMPAR-mediated, but not NMDAR-mediated, EPSCs. Decreased AMPAR synaptic transmission was not associated with a reduction of spine density of CA1 neurons or changes in total GluA1/2 hippocampal levels in HTZ Nlgn1 Thr271fs mice, pointing at decreased synaptic abundance of AMPAR.[14] These results indicate an age-dependent susceptibility of hippocampal AMPAR-mediated synaptic transmission and LTP to reduced levels of Nlgn1.

The age-dependent decrease in AMPAR-mediated synaptic response and LTP in the hippocampus of HTZ Nlgn1 Thr271fs mice was an unexpected finding based on the current knowledge of Nlgn1 in glutamate receptor function. Although Nlgn1 expression in cultured neurons increases NMDAR- and AMPAR-mediated synaptic transmission, several studies have repeatedly found a major decrease in NMDAR-mediated, but not AMPAR-mediated, EPSCs upon inhibition of Nlgn1 in young mice.[11,16–20] These findings might indicate that Nlgn1 is dispensable for AMPAR-mediated synaptic responses *in vivo*. Our data point at an alternative view, where a partial loss of Nlgn1 alters AMPAR-mediated synaptic transmission in an age-dependent manner. The fact that basal synaptic transmission was normal through the life of HMZ Nlgn1 Thr271fs mice could indicate the induction of a compensatory mechanism. It has been shown that expression of Nlgn3 can rescue the decrease in AMPAR-synaptic responses, but not the impairment in NMDAR-currents and in LTP, of Nlgn1-deficient hippocampal neurons.[39,40] Notably, we observed that Nlgn3 specifically increases in the hippocampus of HMZ Nlgn1 Thr271fs mice, providing a clue for the expression of a partly compensatory mechanism, which is not induced upon a partial reduction of Nlgn1. The observation that HTZ Nlgn1 Thr271fs mice showed age-dependent impairment in LTP but normal NMDAR-mediated EPSCs is consistent with the finding that Nlgn1 regulates hippocampal LTP in an NMDAR-independent pathway.[18] Given the pivotal role of AMPAR in synaptic plasticity,[42] decreased AMPAR response could underlie the age-dependent impairment in hippocampal LTP of the HTZ Nlgn1 Thr271fs mice.

The data in this study suggest that the decrease of Nlgn1 levels previously reported in AD patients and in mouse models may play a pathological role in the synaptic and memory deficits associated with AD. Future approaches in which the effects caused by common AD-associated factors, such as Abeta, were to be evaluated in experimental models with decreased Nlgn1 levels would widen our knowledge on the interplay of Nlgn1 with AD.

Altogether, we have generated a knockin mouse that faithfully reproduces the AD-associated Nlgn1 Thr271fs heterozygous mutation. Biochemical, physiological, and behavioral characterization of the HTZ Nlgn1 Thr271fs mouse from a young to an old age identified specific memory deficits and synaptic defects in AMPAR-mediated synaptic transmission and LTP produced by a partial loss of Nlgn1. These defects differed from the synaptic and behavioral impairments produced by a total loss of Nlgn1 in HMZ Nlgn1 Thr271fs mouse, suggesting the expression of compensatory mechanisms that can limit the discovery step when using disease-unrelated mouse models. The relatively large time period extending from the decrease in Nlgn1 to full symptoms expression offers an experimental window to uncover molecular targets, with the aim to attenuate synapse and memory dysfunction in AD.

Limitations of the study

In this study, we have generated a knockin mouse model that reproduces an AD-associated heterozygous frameshift mutation in the *NLGN1* gene, the Nlgn1 Thr271fs mouse. This animal model has allowed us to study the effects associated with a loss of *Nlgn1* throughout life, concluding that a partial loss of Nlgn1

produces specific memory deficits and an age-dependent decrease in basal synaptic transmission and plasticity. However, we have only analyzed synaptic function at the CA3-CA1 synapse in the hippocampus, based on the role of this brain region in different forms of memory. Therefore, it remains to be determined whether synapse function is also affected in other brain regions. The molecular mechanism for the age-dependent decrease in AMPAR response via a partial decrease in Nlgn1 has not been determined in this study and remains to be pursued in future work. Reduced synaptic abundance of AMPAR is one possible explanation, as the total levels of AMPAR subunits and the density of structural synapses are not affected in the hippocampus of HTZ Nlgn1 Thr271fs mice. Furthermore, we have shown in adult and old mice that the memory defects produced by a partial loss of Nlgn1 in HTZ Nlgn1 Thr271fs mice differ from those caused by a total loss of Nlgn1 in HMZ Nlgn1 Thr271fs mice. Based on the age-dependent synaptic deficits of HTZ Nlgn1 Thr271fs mice, future work should aim at studying the progression or appearance of behavioral deficits during aging in this AD-associated mouse model. Our results show interplay of a sustained reduction of Nlgn1 with aging in a mouse model of disease. However, caution should be taken when translating these results to AD in patients, as the impairment of NLGN1 function could be maintained for an extended period of time before the onset of symptoms,[25,30] and it might be associated with additional AD-related factors.[24,26,28,43]

STAR★METHODS

Detailed methods are provided in the online version of this paper and include the following:

- KEY RESOURCES TABLE
- RESOURCE AVAILABILITY
  - Lead contact
  - Materials availability
  - Data and code availability
- EXPERIMENTAL MODEL AND STUDY PARTICIPANT DETAILS
  - Generation of the Nlgn1 Thr271fs mouse line
- METHOD DETAILS
  - Biochemical analysis
  - Behavioral assays
  - Golgi-Cox staining
  - Electrophysiology
- QUANTIFICATION AND STATISTICAL ANALYSIS

SUPPLEMENTAL INFORMATION

Supplemental information can be found online at https://doi.org/10.1016/j.isci.2023.106868.

ACKNOWLEDGMENTS

This work was funded by grants from Ministerio de Ciencia, Innovación y Universidades (RTI2018-101886-B-100) and Junta de Andalucía (PROYEXCEL_00573) to FGS and AM-M, AEI/FEDER (PID2019107677GBI00) and Juan de Andalucía/FEDER (P20_00881) to A.R.-M. and co-funded by ERDF. We thank Sonia Carrasco-Poley for support with NeuN quantification. FA-A was the recipient of a fellowship from Ministerio de Economía, Industria y Competitividad (BES-2016-076579). IM-G was supported by Formación de Profesorado Universitario predoctoral fellowship from Ministerio de Universidades (FPU 17/04283). ER-L was a fellow from V Plan Propio de Investigación (Universidad de Sevilla). CM-C was the recipient of a Garantía Juvenil contract from Universidad de Sevilla. ACS-H received a fellowship from Junta de Andalucía (P11-CVI-7599). The authors thank Drs. María Luz Montesinos and Itziar Benito for advice in the Barnes maze test; Dr. Francisco Morón, from the Genomics and Sequencing facility at IBiS, and Dr. Francisco Martín, from the animal facility at CITIUS (Universidad de Sevilla). The authors wish to give a special thanks to the late Dr. Oscar Pintado for pronuclear injection.

AUTHOR CONTRIBUTIONS

F.A.-A., E.T.-C., E.R.-L., I.M.-G., H.C.-C., C.M.-C., A.C.S.-H., performed research and analyzed data; A.R.-M. designed and supervised research. A.M.-M. designed and supervised research, acquired funding, and wrote the manuscript; F.G.S., conceived, designed, and supervised research, acquired funding and wrote the manuscript. All the authors revised and approved the manuscript for submission.

DECLARATION OF INTERESTS

The authors declare no competing interests.

INCLUSION AND DIVERSITY

We support inclusive, diverse, and equitable conduct of research.

Received: December 12, 2022
Revised: March 31, 2023
Accepted: May 9, 2023
Published: May 13, 2023

REFERENCES

1. DeKosky, S.T., and Scheff, S.W. (1990). Synapse loss in frontal cortex biopsies in Alzheimer's disease: correlation with cognitive severity. Ann. Neurol. *27*, 457–464. https://doi.org/10.1002/ana.410270502.

2. Selkoe, D.J. (2002). Alzheimer's disease is a synaptic failure. Science *298*, 789–791. https://doi.org/10.1126/science.1074069.

3. Terry, R.D., Masliah, E., Salmon, D.P., Butters, N., DeTeresa, R., Hill, R., Hansen, L.A., and Katzman, R. (1991). Physical basis of cognitive alterations in Alzheimer's disease: synapse loss is the major correlate of cognitive impairment. Ann. Neurol. *30*, 572–580. https://doi.org/10.1002/ana.410300410.

4. Van Cauwenberghe, C., Van Broeckhoven, C., and Sleegers, K. (2016). The genetic landscape of Alzheimer disease: clinical implications and perspectives. Genet. Med. *18*, 421–430. https://doi.org/10.1038/gim.2015.117.

5. Südhof, T.C. (2008). Neuroligins and neurexins link synaptic function to cognitive disease. Nature *455*, 903–911. https://doi.org/10.1038/nature07456.

6. Jamain, S., Quach, H., Betancur, C., Råstam, M., Colineaux, C., Gillberg, I.C., Soderstrom, H., Giros, B., Leboyer, M., Gillberg, C., and Bourgeron, T.; Paris Autism Research International Sibpair Study (2003). Mutations of the X-linked genes encoding neuroligins NLGN3 and NLGN4 are associated with autism. Nat. Genet. *34*, 27–29. https://doi.org/10.1038/ng1136.

7. Laumonnier, F., Bonnet-Brilhault, F., Gomot, M., Blanc, R., David, A., Moizard, M.P., Raynaud, M., Ronce, N., Lemonnier, E., Calvas, P., et al. (2004). X-linked mental retardation and autism are associated with a mutation in the NLGN4 gene, a member of the neuroligin family. Am. J. Hum. Genet. *74*, 552–557. https://doi.org/10.1086/382137.

8. Jamain, S., Radyushkin, K., Hammerschmidt, K., Granon, S., Boretius, S., Varoqueaux, F., Ramanantsoa, N., Gallego, J., Ronnenberg, A., Winter, D., et al. (2008). Reduced social interaction and ultrasonic communication in a mouse model of monogenic heritable autism. Proc. Natl. Acad. Sci. USA *105*, 1710–1715. https://doi.org/10.1073/pnas.0711555105.

9. Nakanishi, M., Nomura, J., Ji, X., Tamada, K., Arai, T., Takahashi, E., Bućan, M., and Takumi, T. (2017). Functional significance of rare neuroligin 1 variants found in autism. PLoS Genet. *13*, e1006940. https://doi.org/10.1371/journal.pgen.1006940.

10. Song, J.Y., Ichtchenko, K., Südhof, T.C., and Brose, N. (1999). Neuroligin 1 is a postsynaptic cell-adhesion molecule of excitatory synapses. Proc. Natl. Acad. Sci. USA *96*, 1100–1105. https://doi.org/10.1073/pnas.96.3.1100.

11. Budreck, E.C., Kwon, O.B., Jung, J.H., Baudouin, S., Thommen, A., Kim, H.S., Fukazawa, Y., Harada, H., Tabuchi, K., Shigemoto, R., et al. (2013). Neuroligin-1 controls synaptic abundance of NMDA-type glutamate receptors through extracellular coupling. Proc. Natl. Acad. Sci. USA *110*, 725–730. https://doi.org/10.1073/pnas.1214718110.

12. Heine, M., Thoumine, O., Mondin, M., Tessier, B., Giannone, G., and Choquet, D. (2008). Activity-independent and subunit-specific recruitment of functional AMPA receptors at neurexin/neuroligin contacts. Proc. Natl. Acad. Sci. USA *105*, 20947–20952. https://doi.org/10.1073/pnas.0804007106.

13. Letellier, M., Szíber, Z., Chamma, I., Saphy, C., Papasideri, I., Tessier, B., Sainlos, M., Czöndör, K., and Thoumine, O. (2018). A unique intracellular tyrosine in neuroligin-1 regulates AMPA receptor recruitment during synapse differentiation and potentiation. Nat. Commun. *9*, 3979. https://doi.org/10.1038/s41467-018-06220-2.

14. Letellier, M., Lagardère, M., Tessier, B., Janovjak, H., and Thoumine, O. (2020). Optogenetic control of excitatory post-synaptic differentiation through neuroligin-1 tyrosine phosphorylation. Elife *9*, e52027. https://doi.org/10.7554/eLife.52027.

15. Mondin, M., Labrousse, V., Hosy, E., Heine, M., Tessier, B., Levet, F., Poujol, C., Blanchet, C., Choquet, D., and Thoumine, O. (2011). Neurexin-neuroligin adhesions capture surface-diffusing AMPA receptors through PSD-95 scaffolds. J. Neurosci. *31*, 13500–13515. https://doi.org/10.1523/jneurosci.6439-10.2011.

16. Blundell, J., Blaiss, C.A., Etherton, M.R., Espinosa, F., Tabuchi, K., Walz, C., Bolliger, M.F., Südhof, T.C., and Powell, C.M. (2010). Neuroligin-1 deletion results in impaired spatial memory and increased repetitive behavior. J. Neurosci. *30*, 2115–2129. https://doi.org/10.1523/JNEUROSCI.4517-09.2010.

17. Chubykin, A.A., Atasoy, D., Etherton, M.R., Brose, N., Kavalali, E.T., Gibson, J.R., and Südhof, T.C. (2007). Activity-dependent validation of excitatory versus inhibitory synapses by neuroligin-1 versus neuroligin-2. Neuron *54*, 919–931. https://doi.org/10.1016/j.neuron.2007.05.029.

18. Jiang, M., Polepalli, J., Chen, L.Y., Zhang, B., Südhof, T.C., and Malenka, R.C. (2017). Conditional ablation of neuroligin-1 in CA1 pyramidal neurons blocks LTP by a cell-autonomous NMDA receptor-independent mechanism. Mol. Psychiatr. *22*, 375–383. https://doi.org/10.1038/mp.2016.80.

19. Kim, J., Jung, S.Y., Lee, Y.K., Park, S., Choi, J.S., Lee, C.J., Kim, H.S., Choi, Y.B., Scheiffele, P., Bailey, C.H., et al. (2008). Neuroligin-1 is required for normal expression of LTP and associative fear memory in the amygdala of adult animals. Proc. Natl. Acad. Sci. USA *105*, 9087–9092. https://doi.org/10.1073/pnas.0803448105.

20. Wu, X., Morishita, W.K., Riley, A.M., Hale, W.D., Südhof, T.C., and Malenka, R.C. (2019). Neuroligin-1 signaling controls LTP and NMDA receptors by distinct molecular pathways. Neuron *102*, 621–635.e3. https://doi.org/10.1016/j.neuron.2019.02.013.

21. Gruart, A., Muñoz, M.D., and Delgado-García, J.M. (2006). Involvement of the CA3-CA1 synapse in the acquisition of associative learning in behaving mice. J. Neurosci. *26*, 1077–1087. https://doi.org/10.1523/jneurosci.2834-05.2006.

22. Whitlock, J.R., Heynen, A.J., Shuler, M.G., and Bear, M.F. (2006). Learning induces long-term potentiation in the hippocampus. Science *313*, 1093–1097. https://doi.org/10.1126/science.1128134.

23. Camporesi, E., Lashley, T., Gobom, J., Lantero-Rodriguez, J., Hansson, O., Zetterberg, H., Blennow, K., and Becker, B. (2021). Neuroligin-1 in brain and CSF of neurodegenerative disorders: investigation for synaptic biomarkers. Acta Neuropathol. Commun. *9*, 19. https://doi.org/10.1186/s40478-021-01119-4.

24. Dufort-Gervais, J., Provost, C., Charbonneau, L., Norris, C.M., Calon, F., Mongrain, V., and Brouillette, J. (2020). Neuroligin-1 is altered in the hippocampus of Alzheimer's disease patients and mouse models, and modulates the toxicity of amyloid-beta oligomers. Sci. Rep. *10*, 6956. https://doi.org/10.1038/s41598-020-63255-6.

25. Goetzl, E.J., Abner, E.L., Jicha, G.A., Kapogiannis, D., and Schwartz, J.B. (2018). Declining levels of functionally specialized synaptic proteins in plasma neuronal exosomes with progression of Alzheimer's disease. Faseb. J. *32*, 888–893. https://doi.org/10.1096/fj.201700731R.

26. Brito-Moreira, J., Lourenco, M.V., Oliveira, M.M., Ribeiro, F.C., Ledo, J.H., Diniz, L.P., Vital, J.F.S., Magdesian, M.H., Melo, H.M., Barros-Aragão, F., et al. (2017). Interaction of amyloid-β (Aβ) oligomers with neurexin 2α and neuroligin 1 mediates synapse damage and memory loss in mice. J. Biol. Chem. *292*, 7327–7337. https://doi.org/10.1074/jbc.M116.761189.

27. Dinamarca, M.C., Di Luca, M., Godoy, J.A., and Inestrosa, N.C. (2015). The soluble extracellular fragment of neuroligin-1 targets Aβ oligomers to the postsynaptic region of excitatory synapses. Biochem. Biophys. Res. Commun. *466*, 66–71. https://doi.org/10.1016/j.bbrc.2015.08.107.

28. Bie, B., Wu, J., Yang, H., Xu, J.J., Brown, D.L., and Naguib, M. (2014). Epigenetic suppression of neuroligin 1 underlies amyloid-induced memory deficiency. Nat. Neurosci. *17*, 223–231. https://doi.org/10.1038/nn.3618.

29. Dang, R., Qi, J., Liu, A., Ren, Q., Lv, D., Han, L., Zhou, Z., Cao, F., Xie, W., and Jia, Z. (2018). Regulation of hippocampal long term depression by Neuroligin 1. Neuropharmacology *143*, 205–216. https://doi.org/10.1016/j.neuropharm.2018.09.035.

30. Tristán-Clavijo, E., Camacho-Garcia, R.J., Robles-Lanuza, E., Ruiz, A., van der Zee, J., Van Broeckhoven, C., Hernandez, I., Martinez-Mir, A., and Scholl, F.G. (2015). A truncating mutation in Alzheimer's disease inactivates neuroligin-1 synaptic function. Neurobiol. Aging *36*, 3171–3175. https://doi.org/10.1016/j.neurobiolaging.2015.09.004.

31. Peça, J., Feliciano, C., Ting, J.T., Wang, W., Wells, M.F., Venkatraman, T.N., Lascola, C.D., Fu, Z., and Feng, G. (2011). Shank3 mutant mice display autistic-like behaviours and striatal dysfunction. Nature *472*, 437–442. https://doi.org/10.1038/nature09965.

32. Rabaneda, L.G., Robles-Lanuza, E., Nieto-González, J.L., and Scholl, F.G. (2014). Neurexin dysfunction in adult neurons results in autistic-like behavior in mice. Cell Rep. *8*, 338–346. https://doi.org/10.1016/j.celrep.2014.06.022.

33. Silverman, J.L., Yang, M., Lord, C., and Crawley, J.N. (2010). Behavioural phenotyping assays for mouse models of autism. Nat. Rev. Neurosci. *11*, 490–502. https://doi.org/10.1038/nrn2851.

34. Harrison, F.E., Hosseini, A.H., and McDonald, M.P. (2009). Endogenous anxiety and stress responses in water maze and Barnes maze spatial memory tasks. Behav. Brain Res. *198*, 247–251. https://doi.org/10.1016/j.bbr.2008.10.015.

35. Hammond, R.S., Tull, L.E., and Stackman, R.W. (2004). On the delay-dependent involvement of the hippocampus in object recognition memory. Neurobiol. Learn. Mem. *82*, 26–34. https://doi.org/10.1016/j.nlm.2004.03.005.

36. Cohen, S.J., Munchow, A.H., Rios, L.M., Zhang, G., Asgeirsdóttir, H.N., and Stackman, R.W., Jr. (2013). The rodent hippocampus is essential for nonspatial object memory. Curr. Biol. *23*, 1685–1690. https://doi.org/10.1016/j.cub.2013.07.002.

37. Rampon, C., Tang, Y.P., Goodhouse, J., Shimizu, E., Kyin, M., and Tsien, J.Z. (2000). Enrichment induces structural changes and recovery from nonspatial memory deficits in CA1 NMDAR1-knockout mice. Nat. Neurosci. *3*, 238–244. https://doi.org/10.1038/72945.

38. Tang, Y.P., Shimizu, E., Dube, G.R., Rampon, C., Kerchner, G.A., Zhuo, M., Liu, G., and Tsien, J.Z. (1999). Genetic enhancement of learning and memory in mice. Nature *401*, 63–69. https://doi.org/10.1038/43432.

39. Chanda, S., Hale, W.D., Zhang, B., Wernig, M., and Südhof, T.C. (2017). Unique versus redundant functions of neuroligin genes in shaping excitatory and inhibitory synapse properties. J. Neurosci. *37*, 6816–6836. https://doi.org/10.1523/jneurosci.0125-17.2017.

40. Shipman, S.L., and Nicoll, R.A. (2012). A subtype-specific function for the extracellular domain of neuroligin 1 in hippocampal LTP. Neuron *76*, 309–316. https://doi.org/10.1016/j.neuron.2012.07.024.

41. Clark, R.E., Zola, S.M., and Squire, L.R. (2000). Impaired recognition memory in rats after damage to the hippocampus. J. Neurosci. *20*, 8853–8860. https://doi.org/10.1523/jneurosci.20-23-08853.2000.

42. Malinow, R., and Malenka, R.C. (2002). AMPA receptor trafficking and synaptic plasticity. Annu. Rev. Neurosci. *25*, 103–126. https://doi.org/10.1146/annurev.neuro.25.112701.142758.

43. Servián-Morilla, E., Robles-Lanuza, E., Sánchez-Hidalgo, A.C., Camacho-Garcia, R.J., Paez-Gomez, J.A., Mavillard, F., Saura, C.A., Martinez-Mir, A., and Scholl, F.G. (2018). Proteolytic processing of neurexins by presenilins sustains synaptic vesicle release. J. Neurosci. *38*, 901–917. https://doi.org/10.1523/jneurosci.1357-17.2017.

44. Rogers, D.C., Fisher, E.M., Brown, S.D., Peters, J., Hunter, A.J., and Martin, J.E. (1997). Behavioral and functional analysis of mouse phenotype: SHIRPA, a proposed protocol for comprehensive phenotype assessment. Mamm. Genome *8*, 711–713. https://doi.org/10.1007/s003359900551.

45. Sánchez-Hidalgo, A.C., Arias-Aragón, F., Romero-Barragán, M.T., Martín-Cuevas, C., Delgado-García, J.M., Martinez-Mir, A., and Scholl, F.G. (2022). Selective expression of the neurexin substrate for presenilin in the adult forebrain causes deficits in associative memory and presynaptic plasticity. Exp. Neurol. *347*, 113896. https://doi.org/10.1016/j.expneurol.2021.113896.

46. Andrade-Talavera, Y., Benito, I., Casañas, J.J., Rodríguez-Moreno, A., and Montesinos, M.L. (2015). Rapamycin restores BDNF-LTP and the persistence of long-term memory in a model of Down's syndrome. Neurobiol. Dis. *82*, 516–525. https://doi.org/10.1016/j.nbd.2015.09.005.

47. Glaser, E.M., and Van der Loos, H. (1981). Analysis of thick brain sections by obverse-reverse computer microscopy: application of a new, high clarity Golgi-Nissl stain. J. Neurosci. Methods *4*, 117–125. https://doi.org/10.1016/0165-0270(81)90045-5.

48. Marco, S., Giralt, A., Petrovic, M.M., Pouladi, M.A., Martínez-Turrillas, R., Martínez-Hernández, J., Kaltenbach, L.S., Torres-Peraza, J., Graham, R.K., Watanabe, M., et al. (2013). Suppressing aberrant GluN3A expression rescues synaptic and behavioral impairments in Huntington's disease models. Nat. Med. *19*, 1030–1038. https://doi.org/10.1038/nm.3246.

49. Forster, B., Van De Ville, D., Berent, J., Sage, D., and Unser, M. (2004). Complex wavelets for extended depth-of-field: a new method for the fusion of multichannel microscopy images. Microsc. Res. Tech. *65*, 33–42. https://doi.org/10.1002/jemt.20092.

50. Lyon, L., Borel, M., Carrión, M., Kew, J.N.C., Corti, C., Harrison, P.J., Burnet, P.W.J., Paulsen, O., and Rodríguez-Moreno, A. (2011). Hippocampal mossy fiber long-term depression in Grm2/3 double knockout mice. Synapse *65*, 945–954. https://doi.org/10.1002/syn.20923.

51. Andrade-Talavera, Y., Duque-Feria, P., Paulsen, O., and Rodríguez-Moreno, A. (2016). Presynaptic spike timing-dependent long-term depression in the mouse hippocampus. Cerebr. Cortex *26*, 3637–3654. https://doi.org/10.1093/cercor/bhw172.

52. Falcón-Moya, R., Pérez-Rodríguez, M., Prius-Mengual, J., Andrade-Talavera, Y., Arroyo-García, L.E., Pérez-Artés, R., Mateos-Aparicio, P., Guerra-Gomes, S., Oliveira, J.F., Flores, G., and Rodríguez-Moreno, A. (2020). Astrocyte-mediated switch in spike timing-dependent plasticity during hippocampal development. Nat. Commun. *11*, 4388. https://doi.org/10.1038/s41467-020-18024-4.

53. Pérez-Rodríguez, M., Arroyo-García, L.E., Prius-Mengual, J., Andrade-Talavera, Y., Armengol, J.A., Pérez-Villegas, E.M., Duque-Feria, P., Flores, G., and Rodríguez-Moreno, A. (2019). Adenosine receptor-mediated developmental loss of spike timing-dependent depression in the hippocampus. Cerebr. Cortex *29*, 3266–3281. https://doi.org/10.1093/cercor/bhy194.

STAR★METHODS

KEY RESOURCES TABLE

REAGENT or RESOURCE	SOURCE	IDENTIFIER
Antibodies		
Mouse anti N-terminal Nlgn1	Synaptic Systems	Clone 4C12; Cat# 129 111; RRID: AB_887747
Mouse anti C-terminal Nlgn1	UC Davis/NIH NeuroMab Facility	Clone N97A/31; Cat# N97A/31; RRID: AB_2877345
Mouse anti NL2	Synaptic Systems	Clone 5E6; Cat# 129 511; RRID: AB_2619813
Mouse anti NL3	UC Davis/NIH NeuroMab Facility	Clone N110/29; Cat# N110/29; RRID: AB_2877346
Mouse anti GluA1	Santa Cruz Biotechnology	Cat# sc-55509; RRID: AB_629532
Mouse anti GluA2	UC Davis/NIH NeuroMab Facility	Cat# L21/32; RRID: AB_2877267
Mouse anti-PSD-95	Thermo Fisher Scientific	Cat# MA1-045; RRID: AB_325399
Mouse anti-β actin	Sigma-Aldrich	Cat# A5316; RRID: AB_476743
Mouse anti C-terminal Nlgn1	UC Davis/NIH NeuroMab Facility	Clone N97A/31; Cat# N97A/31; RRID: AB_2877345
Mouse anti NL2	Synaptic Systems	Clone 5E6; Cat# 129 511; RRID: AB_2619813
Mouse anti NL3	UC Davis/NIH NeuroMab Facility	Clone N110/29; Cat# N110/29; RRID: AB_2877346
Mouse anti GluA1	Santa Cruz Biotechnology	Cat# sc-55509; RRID: AB_629532
Mouse anti GluA2	UC Davis/NIH NeuroMab Facility	Cat# L21/32; RRID: AB_2877267
Mouse anti-PSD-95	Thermo Fisher Scientific	Cat# MA1-045; RRID: AB_325399
Mouse anti-β actin	Sigma-Aldrich	Cat# A5316; RRID: AB_476743
Critical Commercial Assays		
RNeasy kit	Qiagen	74104
QuantiTect Reversed Transcription kit	Qiagen	205311
cOmplete Tablets EDTA-free, *EASYpack*	Roche	04693132001
Horseradish peroxidase	Jackson ImmunoResearch Labs	Cat# 115-035-003, RRID: AB_10015289 mouse
Clarity ECL Substrate	Bio-Rad	1705060
Clarity Max ECL Substrate	Bio-Rad	1705062
Experimental Models: Organisms/Strains		
Mouse: Nlgn1 Thr271fs: B6;FVB-*Nlgn1*^{em1Fgs}	This paper	N/A
Oligonucleotides		
RT-PCR forward	5′-ACTACGGGCTCCTTGACCTC-3′	N/A
RT-PCR reverse	5′- GCTATGTGGTATCGGGCTGG -3′	N/A
Genotyping forward	5′- TCCAGGCTTCTTGAGCACAG -3′	N/A
Genotyping reverse	5′- CATCTTACCCAGCTCCATGG -3′	N/A
Software and algorithms		
GraphPad Prism software	Dotmatics	RRID: SCR_002798
BioRender.com	Biorender	RRID: SCR_018361
SMART Video Tracking Software	Panlab, Harvard Apparatus	RRID: SCR_002852
Packwin software	Panlab	N/A
Extended Depth of Field plugin for ImageJ software	ImageJ	RRID: SCR_003070

(*Continued on next page*)

Continued

REAGENT or RESOURCE	SOURCE	IDENTIFIER
pCLAMP 10.2 software	Molecular Devices	RRID: SCR_011323
Clampfit 10.2 software	pCLAMP, Molecular Devices	RRID: SCR_011323
SigmaPlot	Systat Software, Inc	N/A

RESOURCE AVAILABILITY

Lead contact

Further information and requests for resources and reagents should be directed to and will be fulfilled by the lead contact, Francisco G. Scholl (fgs@us.es).

Materials availability

Materials generated in this study can be made available upon request to the lead contact.

Data and code availability

- Experimental data reported in this paper will be shared by the lead contact upon request.
- This paper does not report original code.
- Any additional information required to reanalyze the data reported in this paper is available from the lead contact upon request.

EXPERIMENTAL MODEL AND STUDY PARTICIPANT DETAILS

Generation of the Nlgn1 Thr271fs mouse line

A DNA fragment containing the *Nlgn1* Thr271fs mutation and a silent *Hpa*I site was co-injected into the pronucleus of FVB/N oocyte together with mRNAs coding for TALENT proteins (Life Technologies) flanking the mutation site in the *Nlgn1* allele. Mouse progeny was analyzed by genomic PCR and founder mice were selected after *Hpa*I digestion of the PCR product. The edited *Nlgn1* allele was confirmed in the founder mice by Sanger sequencing. The selected founder mouse line was mated in a C57BL/6J background. A ratio of 2:1 female-to-male was dedicated to mating in order to obtain a large number of animals for the three experimental groups at different ages. RNA was extracted from dissected brain tissue from male and female mice using the RNeasy kit (Qiagen) and retrotranscribed to cDNA with the QuantiTect Reversed Transcription kit (Qiagen). RT-PCR was performed using primers 5'-ACTACGGGCTCCTTGACCTC-3' (forward) and 5'- GCTATGTGGTATCGGGCTGG -3' (reverse). Animals were kept at 22°C on a 12 h dark/light cycle and food and water were provided *ad libitum*. Mice were used according to animal care standards and all protocols were approved by the Committee of Animal Use for Research at the University of Seville (Spain).

METHOD DETAILS

Biochemical analysis

Forebrain tissues from male and female mice were homogenized in lysis buffer (50 mM Tris-HCl pH 7.4; 100 mM NaCl; 5 mM $MgCl_2$; 1% Triton X-100 and 0.1% SDS) containing a protease inhibitor cocktail (Roche). Western blot experiments of lysates containing equal-protein loading (20-40 μg per lysate) were performed using the following primary antibodies: mouse anti N-terminal Nlgn1 (1:1,000, Synaptic Systems, clone 4C12, Cat# 129 111, RRID: AB_887747); mouse anti C-terminal Nlgn1 (1:1,000, UC Davis/NIH NeuroMab Facility Cat# N97A/31, clone N97A/31, RRID: AB_2877345); mouse anti NL2 (1:1,000, Synaptic Systems, clone 5E6, Cat# 129 511, RRID: AB_2619813); mouse anti NL3 (1:1,000, UC Davis/NIH NeuroMab Facility, clone N110/29, Cat# N110/29, RRID: AB_2877346); mouse anti GluA1 (1:500, Santa Cruz Biotechnology, Cat# sc-55509, RRID: AB_629532); mouse anti GluA2 (1:1,000, UC Davis/NIH NeuroMab Facility, Cat# L21/32, RRID: AB_2877267); mouse anti-PSD-95 (1:1,000, Thermo Fisher Scientific, Cat# MA1-045, RRID: AB_325399); and mouse anti-β actin (1:5,000, Sigma-Aldrich, Cat# A5316, RRID: AB_476743). Immunoreactivity was detected with appropriate secondary antibodies conjugated with horseradish peroxidase (1:5,000, Jackson ImmunoResearch Labs, Cat# 115-035-003, RRID: AB_10015289 mouse). Chemiluminescence was developed using Clarity ECL Substrate (Bio-Rad) or Clarity Max ECL Substrate (Bio-Rad) on a ChemiDoc Touch Imaging System (BioRad ChemiDoc Touch Imaging System, RRID: SCR_021693).

Behavioral assays

Male mice were tested at 4-8 months unless otherwise specified. Experienced researchers unaware of the mice genotype performed all experimental tests and their quantitation. For all animals, general health was checked following the SHIRPA procedure, including locomotion and neurological reflexes.[44] All data were analyzed using GraphPad Prism software (Dotmatics, RRID: SCR_002798). Data were subjected to Shapiro-Wilk normality and equal variance tests. Statistical comparisons were performed as described in the corresponding figure legend for each experiment. Data are presented as mean ± SEM. P-values are indicated in the figure legends. P-values less than 0.05 were considered statistically significant. Schematic drawings of behavioral tests were created with Biorender.com (RRID: SCR_018361).

Open field

The tested mouse was allowed to freely explore a square open field arena (45 x 45 cm, Harvard Apparatus) for 15 min. Automatic detection of the mouse, total traveled distance and time spent in the central zone (20 cm apart from the walls) were recorded with the SMART Video Tracking Software (Panlab, Harvard Apparatus, RRID: SCR_002852). A minimal travel distance of 2,000 cm was applied as an inclusion criterion. Averaged age of tested mice, 4.35 ± 0.09 months (Figure S2A).

Self-grooming

Stereotyped behavior was studied with the self-grooming test. Mice were placed in a clean cage without bedding. After 10 min of habituation, behavior was video-recorded for 10 min. Time spent in self-grooming and number of bouts were manually quantified. A minimal self-grooming time of 10 sec was set as an inclusion criterion. Averaged age of tested mice, 4.31 ± 0.09 months (Figure S2B).

Three-chamber test

The test was performed as described previously[33,45] with minor modifications. A social interaction box (Harvard Apparatus) divided in 3 compartments was used. The social arena was made of a transparent box (42 x 60 cm) with two transparent sliding doors that divide left, right and center chambers (42 x 20 cm). During the first 10-minutes session, the tested mouse was placed in the central chamber with the sliding doors closed. Then, a 10-minutes habituation session proceeded where the tested mouse had access to the sided chambers, containing two empty circular cages (8 cm diameter). After habituation, circular cages housing an unfamiliar C57BL/6J mouse of the same sex and age or an inanimate object (plastic cube) was located at the corners of the left or right chamber. A cylindrical bottle filled with water was placed on top of the enclosures to prevent the tested mouse from climbing. The tested mouse was located in the central chamber and allowed to explore the arena for 10 min. The location of the cages was alternated between tests. Mice that did not enter the side chambers during the habituation or the test phases were not further analyzed. Tests were video-recorded and the time spent in close contact with the cages was manually measured. Averaged age of tested mice, 5.22 ± 0.10 months (Figure S2C).

Novel object recognition

The object recognition test comprised a sample phase and a test session, separated by a delay. The delays between the sample and the test sessions used in this study were 5 min, 15 min, 30 min, or 1 h. The mouse was placed in the center of the open field arena and allowed to freely explore the area for 15 min. After the habituation session, two identical objects were placed at opposite corners, 15 cm apart from the walls. The tested mouse was placed back in the center of the field and allowed to explore the objects for 10 min. After the initial presentation, one of the familiar objects was replaced for a new object of similar size but different color and shape. Then, the tested mouse was placed in the arena and allowed to interact with the objects for 10 min. The location of the new object was alternated between assays. Different pairs of objects were randomly assigned and used in each experiment. The objects were cleaned immediately after use to remove olfactory clues. For the study of recognition memory at short delays (5, 15 and 30 min), each experiment was separated by 7 days. The tests were video-recorded and the time spent interacting with the novel or familiar object was manually measured. Preference index per each mouse was calculated as (time interacting with the new object-time interacting with the familiar object)/ total interaction time. Averaged age of tested mice, 4.18 ± 0.12 months (Figure 3), 6.01 ± 0.26 months (Figures 4A), 6.20 ± 0.27 months (Figures 4B), 6.40 ± 0.26 months (Figure 4C).

Barnes maze

The Barnes maze assay was performed as previously described.[45,46] Briefly, mice were located on top of an elevated round platform (Harvard Apparatus) delimited by 20 evenly spaced holes in the periphery. To assess spatial memory, visual-spatial cues were located hanging on panels in the proximity surrounding the platform. During learning, all holes but one, the escape hole, were covered and mice were exposed to the platform. Bright light and standing fans served as motivating factors to induce scape behavior. The escape hole was maintained at a fixed location for the duration of the training, which involved four daily trials (maximum time to find the escape hole: 180 s per trial). In unsuccessful trials, mice were gently guided to the escape hole at the end of the trial. Twenty-four hours after training, mice were tested in a single session of 90 s in the same set-up with all holes covered. The time in reaching the escape hole and spent in each quadrant was automatically quantified (SMART Video Tracking Software, Panlab, Harvard Apparatus, RRID: SCR_002852). Averaged age of tested mice, 8.59 $\pm$ 0.05 months (Figure 2A).

Fear conditioning

Fear conditioning was evaluated in a test box (Harvard Apparatus) as previously described.[45] Briefly, mice were allowed to freely explore the test box for 2 min before they were exposed to conditioning phase consisting of three repetitions of a 30 s tone co-terminating with a mild electric shock (0.2 mA). After 24 h, mice were exposed to three repetitions of the tone but in a different colored and shaped chamber and without a shock. Freezing response during the tests was detected with sensors located on the floor. Packwin software (Panlab) was used to automatically analyze the freezing response. Averaged age of tested mice, 9.64 $\pm$ 0.09 months (Figure 2A).

Golgi-Cox staining

The Golgi-Cox staining was performed as described previously.[47,48] Briefly, the Golgi-Cox solution (1% $K_2Cr_2O_7$, 1% $HgCl_2$, 0.8% K_2CrO_4) was prepared before its use. Mice were deeply anesthetized with sodium thiopental and decapitated. The brain hemispheres were immersed in the Golgi-Cox solution during three weeks followed by incubation with 90% ethanol for 30 minutes. Coronal brain sections of 200μm thickness obtained in a vibratome were incubated with 15% ammonia and 1% thiosulfate. Brain sections were dehydrated in an ethanol-isopropanol-xylol sequence and mounted in Superfrost-Plus slides with DPX mounting media. Z-stacks images of a 0.5 μm step size containing the full dendritic arbor of CA1 stained neurons were acquired in a BX-61 bright-field microscope (Olympus) with a 100x objective. The number of dendritic spines was manually counted in a known length of secondary dendritic segments using the Extended Depth of Field plugin for ImageJ software (ImageJ, RRID: SCR_003070).[49,50] The density of dendritic spines was calculated for each dendritic segment and averaged for each experimental group.

Electrophysiology

Preparation of hippocampal slices

Hippocampal slices were prepared as follows. Mice were anesthetized with isoflurane (2%) and decapitated for slice preparation. After decapitation, the whole brain, containing the two hippocampi, was removed into ice-cold solution (I) consisting of (in mM): 126 NaCl, 3 KCl, 1.25 KH_2PO_4, 2 $MgSO_4$, 2 $CaCl_2$, 26 $NaHCO_3$, and 10 glucose (pH 7.2, 300 mOsmL-1), positioned on the stage of a vibratome slicer and cut to obtain transverse hippocampal slices (350 mm thick; LEICA VT1000S), which were continuously oxygenated for at least 2 h before use. All experiments were carried out at 30–34°C, during which the slices were continuously perfused with solution I.[51–53]

Electrophysiological recordings

Field excitatory postsynaptic potentials (fEPSPs) were recorded in the CA1 region of the hippocampus of wild-type and Nlgn1 Thr271fs (HTZ and HMZ) mice, divided into three age groups: 4-6, 12-14 and 18-22 months old. fEPSPs in the CA1 region of the hippocampus were evoked with a stimulating electrode placed on the Schaffer collateral (0.2 Hz) using brief current pulses (200 μs, 0.1–0.2 mA). Extracellular recording electrodes were filled with solution I. Stimulation was adjusted to obtain a fEPSP peak amplitude of approximately 1 mV during control conditions. After a stable fEPSP baseline period of 10 min, LTP was induced by a standard protocol consisting of 2 trains of stimuli at 100 Hz for 1 s separated by 20 s. Recordings lasted 120 min after LTP induction. Data were filtered at 3 kHz and acquired at 10 kHz using pCLAMP 10.2 software (Molecular Devices, RRID: SCR_011323). A stimulus-response curve (0.1–0.6 mA, mean of five fEPSPs at each stimulation strength) was compiled for the different mice used. For paired-pulse ratio (PPR)

experiments, two fEPSPs were evoked 40 ms apart for 0.5 min at baseline frequency (6 times) at the beginning of the baseline recording. The PPR was expressed as the slope of the second fEPSP divided by the slope of the first fEPSP.

Whole-cell voltage-clamp recordings were performed from CA1 pyramidal neurons. From the same cell and stimulation, AMPAR and NMDAR excitatory postsynaptic currents (EPSCs) were evoked at -70 and + 40 mV holding potential, respectively. Input-output curves in patch-clamp experiments were performed at -70 mV.

Data analysis

Data were analyzed using Clampfit 10.2 software (pCLAMP, Molecular Devices, RRID: SCR_011323). Data are presented as mean ± SEM. To estimate changes in synaptic efficacy, E-LTP was quantified by comparing the mean fEPSP slope over the 60 min post-tetanus period with the mean fEPSP slope during the baseline period and calculating the percentage change from the 10 last minutes. L-LTP was quantified in the same way but at 120 minutes after the protocol. Graphs were obtained using SigmaPlot 14.0.

Before applying any statistical comparison, the data were subjected to Shapiro-Wilk normality and equal variance tests. For any comparisons between two groups, two-paired Student's t-test was used. For multiple comparisons to the same control, One-way ANOVA and Holm-Sidak test was used. P-values less than 0.05 were considered statistically significant.

QUANTIFICATION AND STATISTICAL ANALYSIS

Statistical analyses were performed using two-paired Student's t-test, one-way or two-way ANOVA with post-hoc analysis, as indicated in each figure legend. A p-value <0.05 was considered significant and the exact p-values are included in the figure legends. Data are presented as mean ± SEM.